

FORCED COOLING OF UNDERGROUND
ELECTRIC POWER TRANSMISSION LINES
PART III OF IV

THE PREDICTION OF FRICTION FACTORS IN TURBULENT
FLOW FOR AN UNDERGROUND FORCED COOLED PIPE-TYPE
ELECTRICAL TRANSMISSION CABLE SYSTEM

by

Joseph W. Beckenbach, Jr.

Leon R. Glicksman

Warren M. Rohsenow

Energy Laboratory
in association with
Heat Transfer Laboratory,
Department of Mechanical Engineering
MASSACHUSETTS INSTITUTE OF TECHNOLOGY

Sponsored by
Consolidated Edison Co. of New York, Inc.
New York, New York

Energy Laboratory Report No. MIT-EL 74-005
Heat Transfer Laboratory Report No. 80619-89

September 1974



ABSTRACT

Forced cooled systems for underground, oil filled, pipe-type electrical transmission cable systems are becoming increasingly common in large urban centers. In systems of this type there exist a number of electrical transmission cables in an oil filled conduit. These cables are wrapped with a semi-circular, protective skid wire, which increases the turbulence in the flow and up until now has prevented any accurate or realistic prediction of the pressure drop. An equation has been used which correlates the friction factor of the rough surface which has been developed which combines the effects of the rough and smooth surface on the flow to obtain a friction factor vs. Reynolds Number plot for the entire pipe-type cable system. This theory has been written in the form of a FORTRAN IV computer program which accepts as input the geometrical dimensions of a system and yields as output the friction factor and corresponding Reynolds Number for the entire pipe-type cable geometry. The results predicted from the theory are consistently 15-30% above the experimentally determined values.

ACKNOWLEDGEMENTS

The authors wish to express their thanks for the generous support of the Consolidated Edison Company of New York who sponsored this work. The helpful assistance of Dr. H. Feibus and Mr. M.D. Buckweitz of Consolidated Edison is also greatly acknowledged.

TABLE OF CONTENTS

	<u>Page</u>
TITLE PAGE.....	1
ABSTRACT.....	2
ACKNOWLEDGMENTS.....	3
TABLE OF CONTENTS.....	4
LIST OF SYMBOLS.....	6
LIST OF TABLES.....	9
LIST OF FIGURES.....	10
CHAPTER I. INTRODUCTION.....	13
CHAPTER II. PREVIOUS WORK.....	17
Hall Transformation.....	17
CHAPTER III. DERIVATION OF METHOD FOR A SIMPLE ANNULUS.....	24
Definition of the Problem.....	24
Friction Factor Correlation for the Rough Surface(cables).....	26
Friction Factor Correlation for the Smooth Surface(pipe).....	30
Combination of Smooth and Rough Surface Friction Correlations to Obtain an Overall Friction Factor vs. Reynolds Number Plot.....	33
CHAPTER IV. COMPARISON OF THEORY WITH EXPERIMENT FOR FLOW IN TUBES AND ANNULAR TYPE GEOMETRIES.....	38
Test of Rough Surface Friction Correlation.....	38
Test of Modified Hall Transformation.....	38
CHAPTER V. EXTENSION OF METHOD FROM ANNULAR TO PIPE-TYPE CASE.....	46
CHAPTER VI. COMPARISON OF THEORY WITH EXPERIMENT FOR FLOW IN A PIPE-TYPE SYSTEM.....	54

TABLE OF CONTENTS (CONT.)

	<u>Page</u>
CHAPTER VII. CONSIDERATION OF THE EFFECTS ON THE FLOW WHEN A POINT OF CONTACT OCCURS.....	57
CHAPTER VIII. PARAMETRIC STUDY.....	70
CHAPTER IX. RESULTS AND CONCLUSIONS.....	81
CHAPTER X. RECOMMENDATIONS.....	83
CHAPTER XI. REFERENCES.....	84
APPENDIX A. FLOW CHART OF COMPUTER PROGRAM.....	87
APPENDIX B. DEFINITION OF VARIABLES USED IN PROGRAM.....	89
APPENDIX C. USER INSTRUCTIONS FOR PROGRAM.....	95
APPENDIX D. SOURCE LISTING.....	97

LIST OF SYMBOLS

- A - cross sectional flow area
- D_c - diameter of cable - to base of skid wire
- D_p - inside diameter of pipe
- D_H - hydraulic diameter = $4 \frac{A}{P}$
- e - height of roughness element
- f - friction factor = $\frac{D_H (dp/dx)}{2\rho v^2}$
- L - length
- P - wetted perimeter
- p - distance between repeated ribs
- dp/dx - pressure gradient
- Re - Reynolds Number = $\frac{VD_H}{\nu}$
- \bar{V} - average bulk fluid velocity
- e^+ - roughness Reynolds Number = $\left(\frac{e}{D_c}\right) Re_1 \sqrt{f_1/2}$
- u - velocity of fluid
- r - radius from center of annuli
- Pr - Prandtl Number = $c_p \mu / k$
- c_p - specific heat at constant pressure
- k - thermal conductivity
- C - wetted circumference
- \dot{m} - mass flow rate
- b - constant

SUBSCRIPTS:

- 1 - pertains to flow in zone 1, influenced by rough cable geometry
- 2 - pertains to flow in zone 2, influenced by smooth pipe geometry
- 3 - pertains to flow in zone 3, influenced by rough cable geometry
- 4 - pertains to flow in zone 4, influenced by smooth pipe geometry
- 12 - pertains to flow in combined zone 1 and 2
- 34 - pertains to flow in combined zone 3 and 4
- T - pertains to flow in total pipe-type cable arrangement
- max - maximum value
- ul - upper limit
- L - pertains to flow in a laminar zone at a point of contact
- o - designates reference position

GREEK SYMBOLS:

α - helix angle

β - half angle of triangular shaped duct

ρ - density

μ - absolute or dynamic viscosity

ν - kinematic viscosity = μ/ρ

τ - shear stress

LIST OF TABLES

	<u>Page</u>
Table 1 NUMBER OF SKID WIRE STARTS AND CORRESPONDING HELIX ANGLE.....	72
Table 2 VARYING THE PITCH, p.....	73
Table 3 DATA CARD ASSEMBLY.....	96

LIST OF FIGURES

	<u>Page</u>
Figure 1 Schematic of Pipe-Type Cable Geometry.....	14
Figure 2 Schematic of Pipe Geometry Investigated by Sams[14] and Eckert[17].....	18
Figure 3 Schematic of Pipe Geometry Investigated by Sams[15].....	19
Figure 4 Schematic of Annuli Investigated by Sheriff & Gumley.....	20
Figure 5 Schematic of Annuli Investigated by Kjellstrom & Hedberg[8] and Feurstein & Rampf[20].....	21
Figure 6 Schematic of Velocity Distribution in an Annular Type Geometry with Inner Surface Rough and Outer Surface Smooth.....	22
Figure 7 Experimentally Determined Values of Friction Factor vs. Reynolds Number for a Pipe-Type Cable System[1].....	25
Figure 8 Ratio of Friction Factor for a Helically Wound Square Wire to Friction Factor for a Transverse Square Rib vs. Helix Angle α , from Wilkie[4].....	28
Figure 9 Ratio of Friction Factro for a Helically Wound Circular Wire to Friction Factor for a Transverse Square Rib vs. Helix Angle α , from Wilkie[3,4].....	29
Figure 10 Friction Factor vs. Reynolds Number for a Smooth Circular, empty pipe. Moody.[18].....	31
Figure 11 Cross Section of Annular Type Geometry.....	35
Figure 12 Comparison of Experimental Data Obtained From a Roughened Tube Similar to the One Shown in Figure 3 with Theoretically Predicted Values. Data is from Sams[15].....	39
Figure 13 Comparison of Predicted Values of Roughness Friction Factor with Experimental Data for a Concentric Annuli Similar to the One Shown in Figure 9. Data is from Sheriff & Gumley[9].....	41

LIST OF FIGURES (CONT.)

	<u>Page</u>
Figure 14 Comparison of Predicted Values of Total Friction Factor with Experimental Data for a Concentric Annuli Similar to the one Shown in Figure 10. Data is from Kjellstrom & Hedberg[8].....	43
Figure 15 Comparison of Predicted Values of Total Friction Factor with Experimental Data for a Concentric Annuli Similar to the one Shown in Figure 5. Data is from Feurstein & Rampf[20]. (e=1 mm.).....	44
Figure 16 Comparison of Predicted Values of Total Friction Factor with Experimental Data for a Concentric Annuli Similar to the one Shown in Figure 5. Data is from Feurstein & Rampf[20]. (e=2 mm.).....	45
Figure 17 Various Pipe-Type Configurations Modelled Shown Divided into Theoretical Flow Zones (dashed lines).....	47
Figure 18 Friction Factor vs. Reynolds Number for Pipe-Type Cable System. Experimental points are for scale model. Predicted values are for full scale system.....	55
Figure 19 Cable-Cable Contact Point Showing Idealized Triangular Duct.....	58
Figure 20 Cable-Pipe Contact.....	58
Figure 21 Co-Ordinate System of Triangular Duct.....	59
Figure 22 Two Infinite Parallel Plates Separated by Distance w.....	59
Figure 23 Theoretically Predicted Values when Points of Contact are Modelled as Laminar Zones.....	69
Figure 24 Theoretically Predicted Results of Varying the Diameter of the Cable, D_c , in a Pipe-Type Cable Geometry.....	71
Figure 25 Theoretically Predicted Results of Varying the Helix Angle, α , in a Pipe-Type Cable Geometry.....	74

LIST OF FIGURES (CONT.)

	<u>Page</u>
Figure 26 Theoretically Predicted Results of Varying the Pitch, p , in a Pipe-Type Cable Geometry.....	76
Figure 27 Theoretically Predicted Results of Varying the Height of the Skid Wire, e , in a Pipe- Type Cable Geometry.....-.....	77
Figure 28 Theoretically Predicted Results of Varying e while Keeping p/e constant in a Pipe-Type Cable Geometry.....	78

CHAPTER I
INTRODUCTION

High pressure, oil filled, underground pipe-type electrical transmission cable systems have been in use for a number of years and are becoming increasingly widespread in large urban areas (figure 1). Originally, the oil was not circulated through the system, and the heat generated by the cables was transferred by natural convection currents in the oil from the cables to the outer pipe wall where it was conducted through the soil to the atmosphere. As the rate of heat generation by the cables increases, the rate of heat transfer out of the system also increases along with a rise in the temperature of the cables, until, ultimate failure.

Since the maximum current carrying capacity of the cables is a function of the heat transfer rate out of the system, and this in turn is a function of the temperature gradient, it is evident that this design has a very undesirable limitation which is the conductive resistance of the soil. To circumvent this problem chilled oil is pumped through the system. Now most of the heat generated by the cables is transferred to the oil and then to the atmosphere at refrigeration stations. However, this new design introduced crucial design problems.

Since this new system requires more capital to build than the static one, it is important to know how to predict the optimum overall design given certain input information. Of paramount importance is the ability to accurately predict the pressure drop of any pipe-type cable system. This is complicated by the fact that the cables have semi-circular, helically wound skid wires wrapped around them which protect the cables as they are being inserted into the pipe.

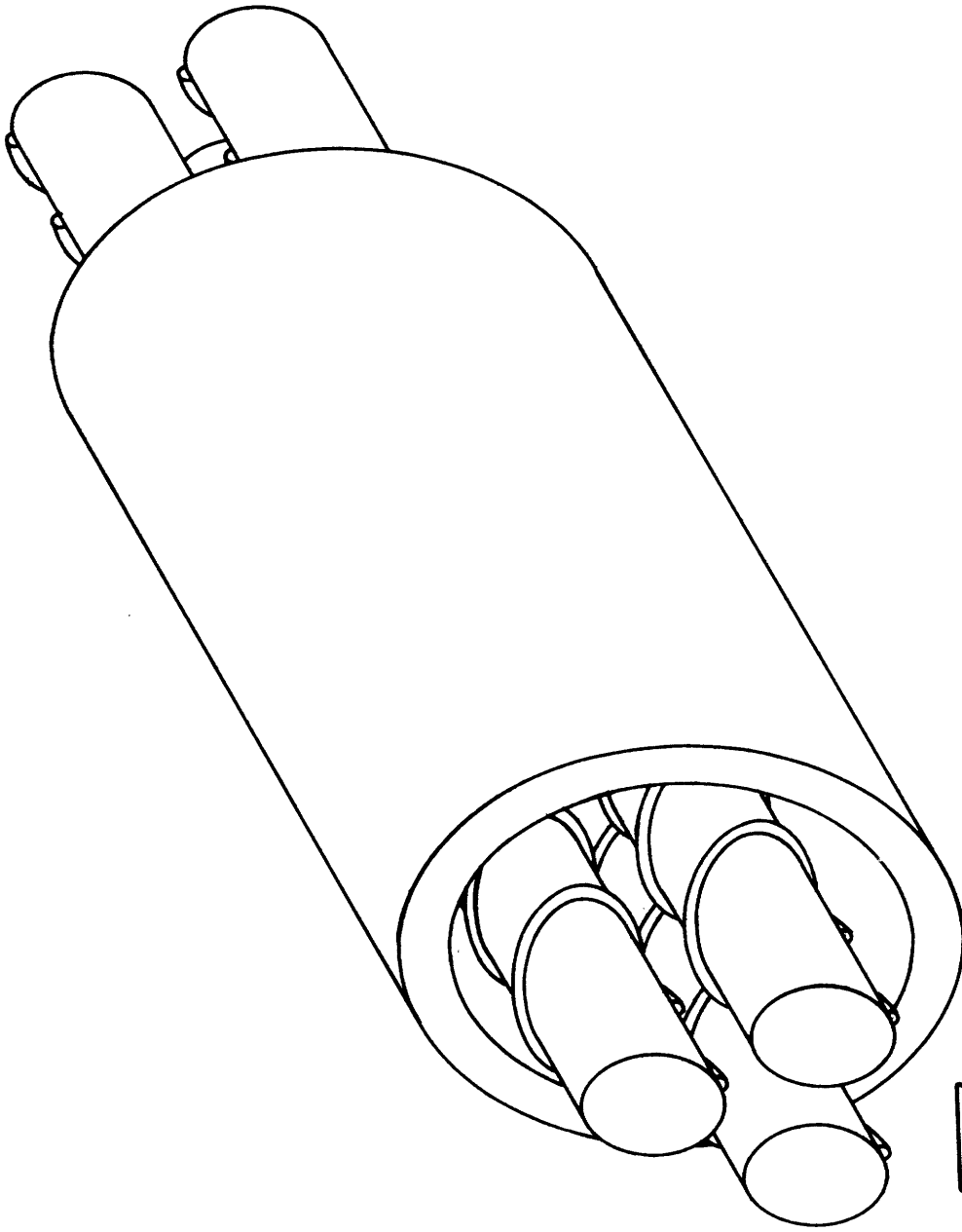


Figure 1. Schematic of Pipe-Type Cable Geometry

↑
OIL MOLT
E

This thesis is concerned with predicting the pressure drop for a specified pipe-type cable geometry size in terms of a friction factor vs. Reynolds number curve for the turbulent flow regime.

The only work to date in this area has been the experimental tests performed at M.I.T.'s Heat Transfer Laboratory [1]. Results showed that due to the increased turbulence created by the skid wires, turbulent flow exists for a Reynolds number as low as 500, based on the hydraulic diameter. This value is approximately in the operating range of interest.

At the present time, there exists no general theory or correlation for the friction factor for the type of rough surface created by the skid wire. There has, however, been a great deal of research carried out especially during the last 15 years on roughness geometries of this type which have been advocated for use on nuclear fuel rods in advanced gas cooled reactors as a means of creating turbulence and increasing the heat transfer rate [2 - 12]. The major results of these experimental investigations have been used, along with a general theory to predict the friction factor for the present case. Four different geometrical arrangements of cable have been modelled. The model for each type of arrangement is described and results are compared with experimental data.

A model which theorizes that the flow at points of contact between two cables behaves like the flow in a narrow, triangular, open ended duct is explained and developed.

Chapter II reviews the important work previously carried out on roughness geometries of the type considered here. Chapter III derives the basic method for a simple annular type geometry, and Chapter IV compares the predictions with experimental data. Chapter V extends the method from

the annular case to the pipe-type case and Chapter VI compares these predictions with experiment. Chapter VII develops a model which theorizes that the points of contact between two cables behaves like the flow in a narrow, triangular, open ended duct. Chapter VIII presents a parametric study of the method developed in Chapter V. Results and conclusions are presented in Chapter IX, and recommendations are suggested in Chapter X. Those only interested in the results may turn directly to Chapter VIII.

PREVIOUS WORK

One of the pioneers in the investigation of discrete roughnesses was W.F. Cope [13], who, in 1941 investigated the effects of small pyramid type proturbances machined in the wall of a pipe. Most of the other work since then has been concerned with improving the performance of nuclear fuel rods in advanced gas cooled reactors by the use of these turbulence promoters. E.W. Sams was probably the first to experiment transverse square ribs and helical coiled wires on the inside surfaces of tubes (1952, 1957)[14, 15] (Fig. 2 & 3).

The difficulty in manufacturing roughness geometries in tubes of this type plus the fact that the turbulence promoters would have to be placed on the outside surface of the fuel elements which in turn are placed in the center of a smooth channel, necessitated a method which could isolate the effects of a rough surface from a smooth surface when they are place opposite one another. In 1958, W.B. Hall [2] proposed such a theory now known as the Hall Transformation. Since this date, most of the research that has been performed on roughened surfaces has been carried out on annular passages with the inner surface roughened, the outer surface smooth, (Fig. 4 & 5), and have used a modified form of the Hall Transformation to correlate the results. Most of the work has been carried out by the United Kingdom Atomic Energy Authority (UKAEA) in England for use on their advanced gas cooled reactor fuel elements.

Hall Transformation

Given a channel which is composed of a rough surface opposite a smooth surface, the idea is to isolate the effects that each one has on the flow. For an annular channel (similar to the one shown schematically

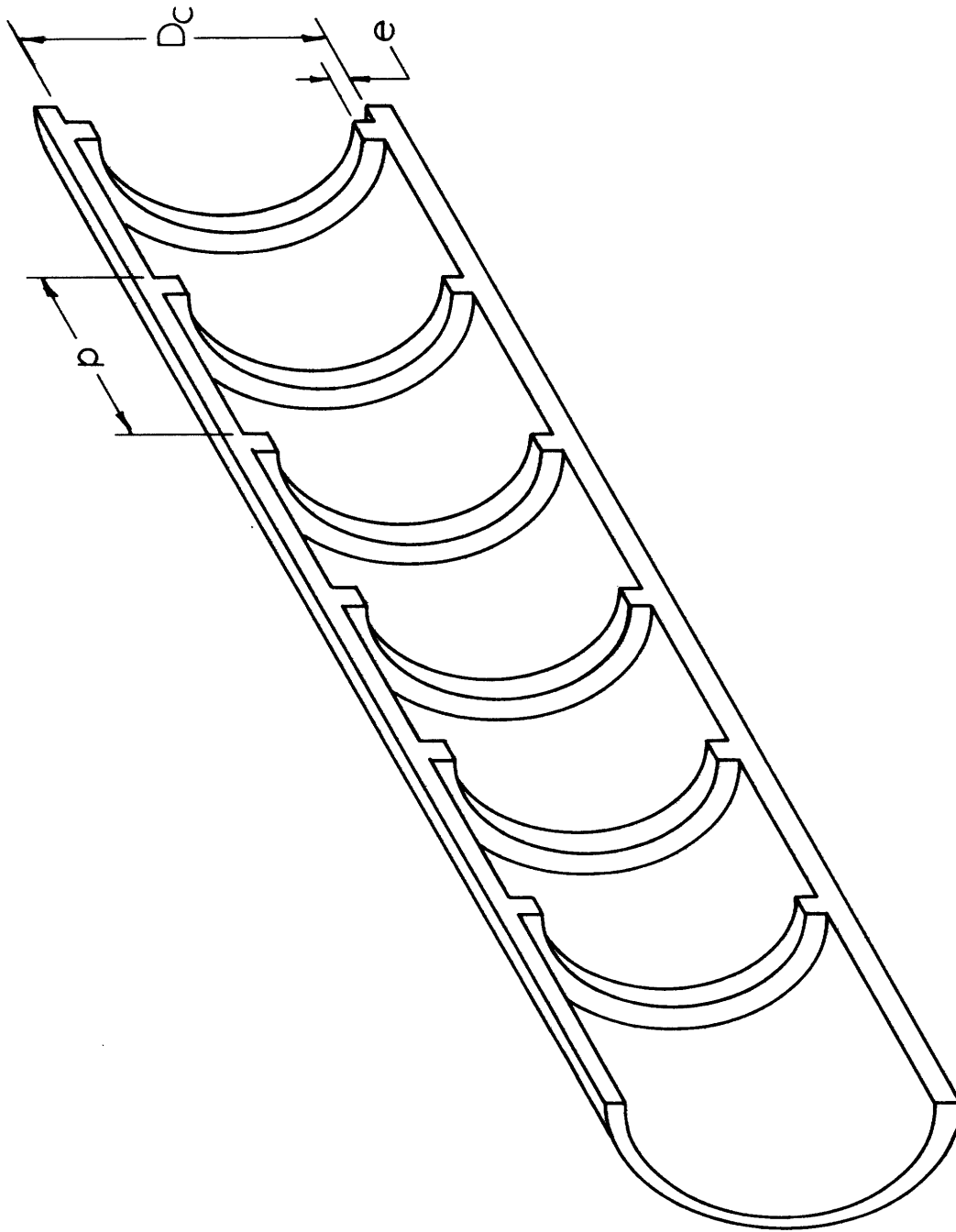


Figure 2. Schematic of Pipe Geometry Investigated by Sams[14] & Eckert[17].

For Sams: $0.46 < p/e < 0.68$

For Eckert: $10 < p/e < 40$

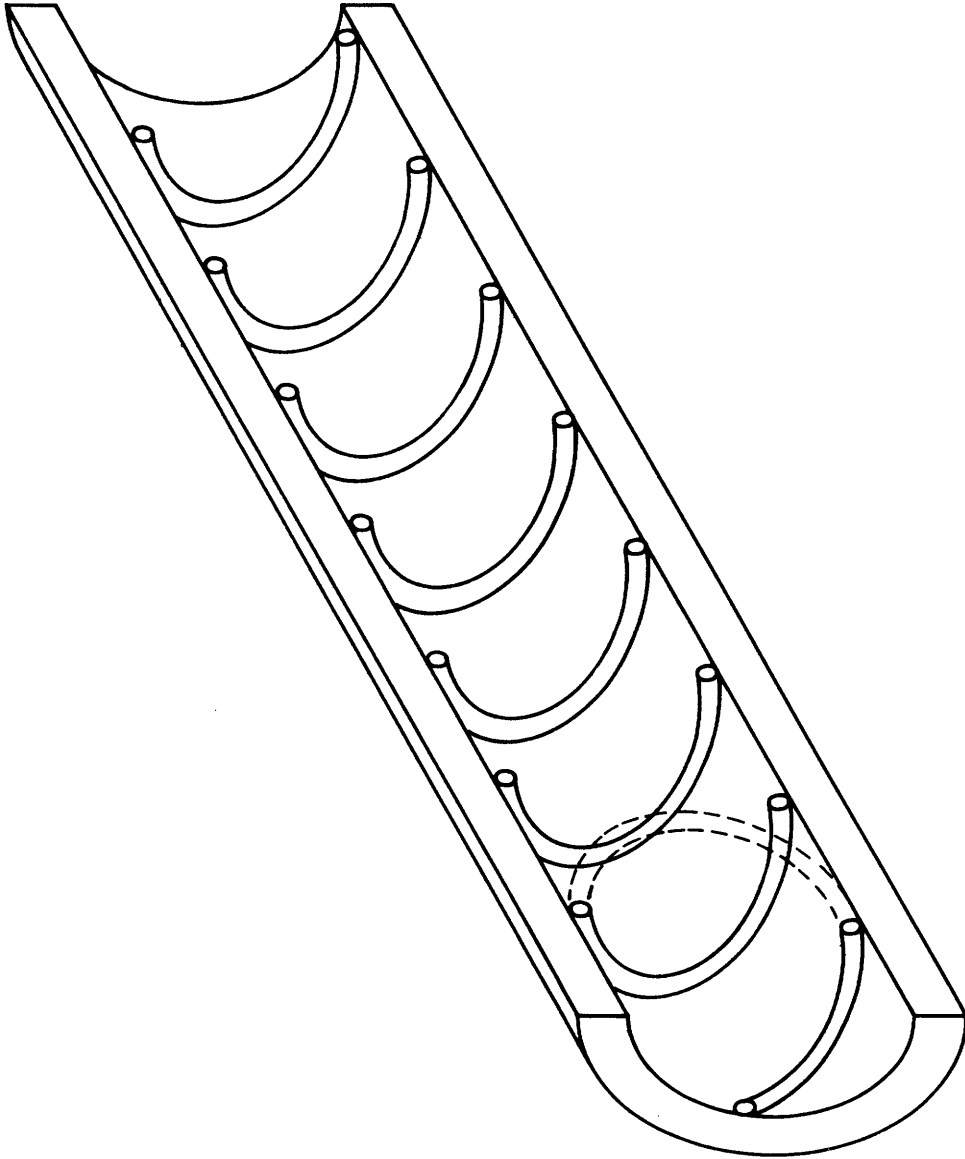


Figure 3. Schematic of Pipe Geometry Investigated by Sams[15].

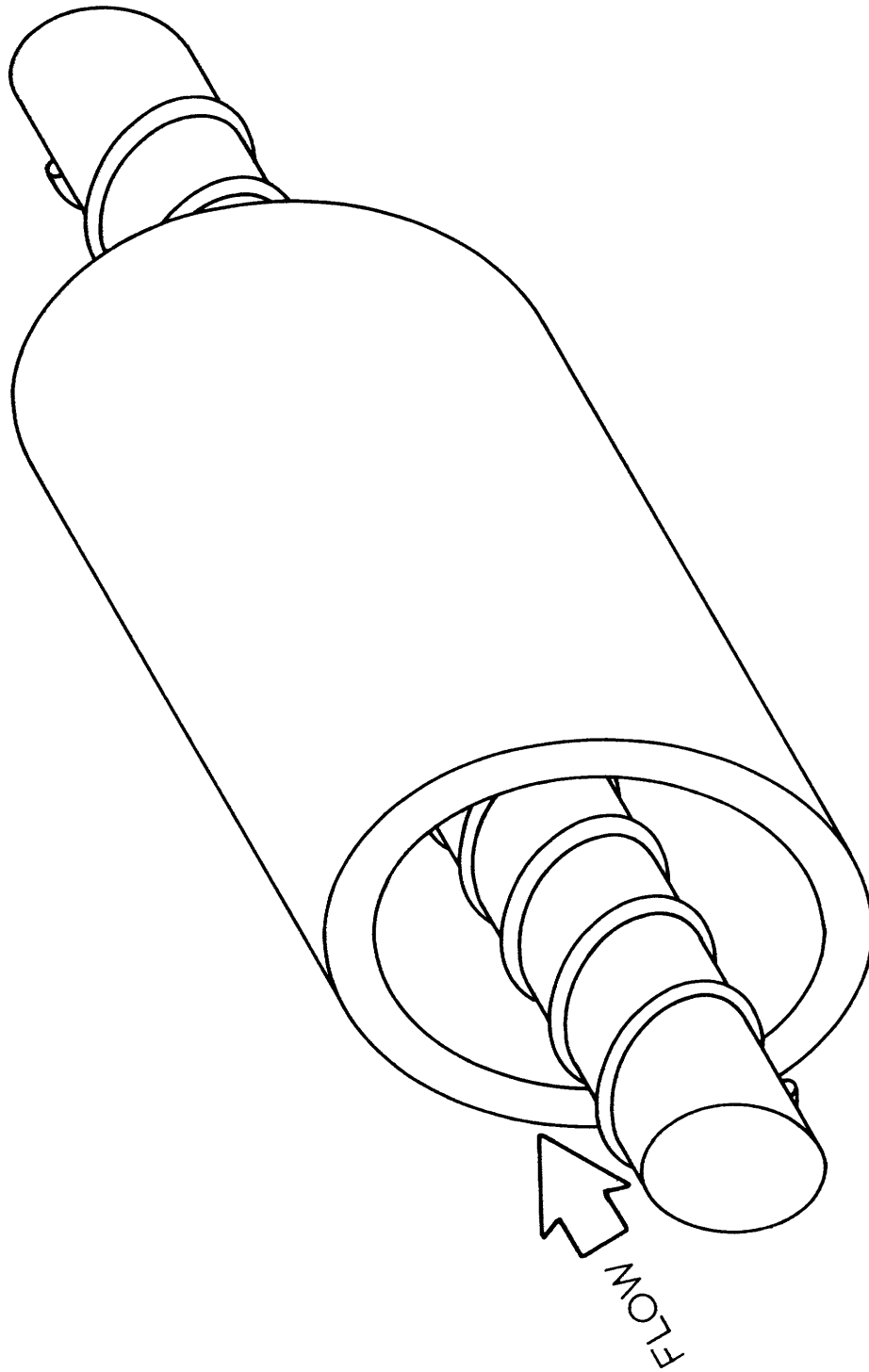


Figure 4. Schematic of Annuli Investigated by Sheriff & Gumley[9]

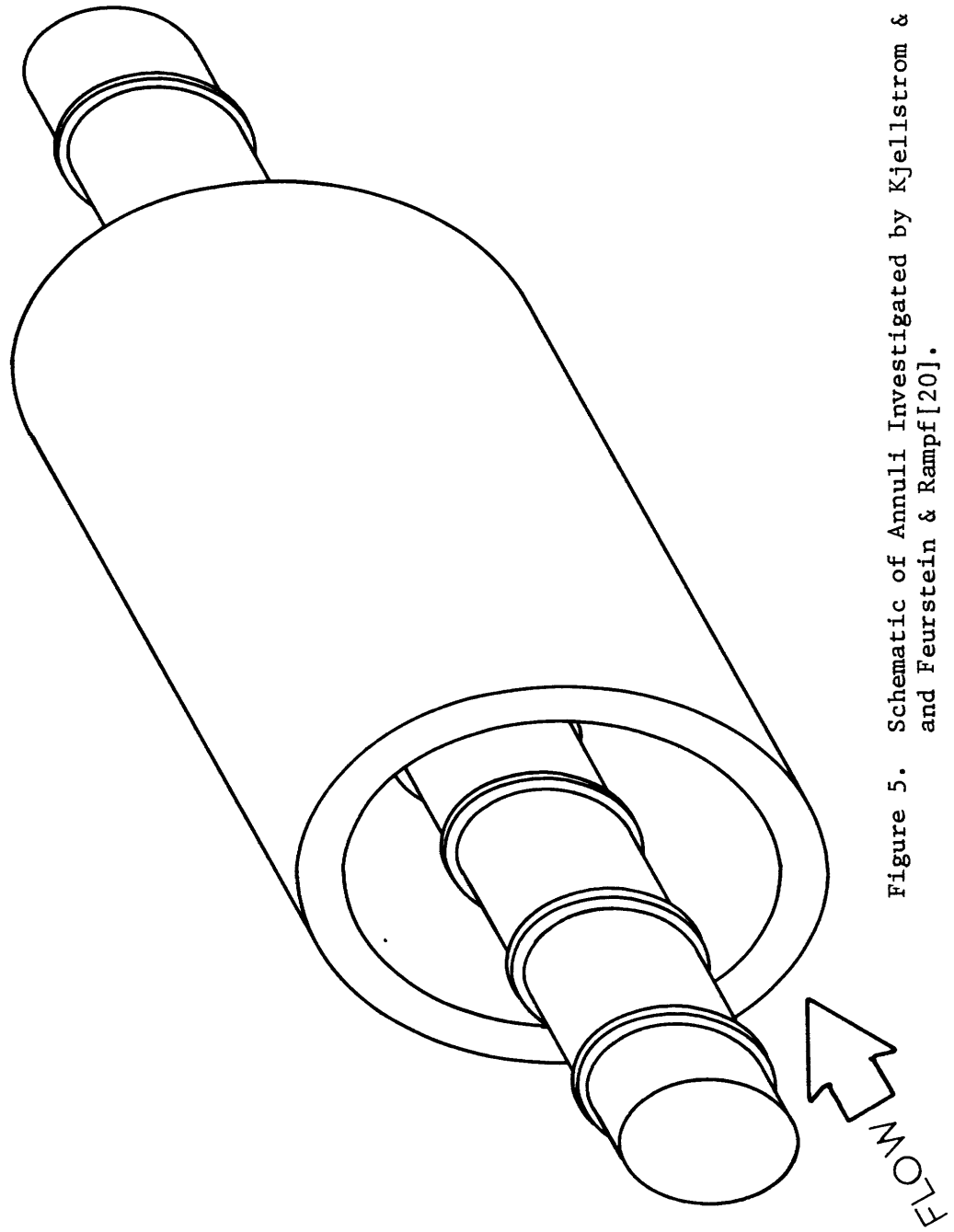


Figure 5. Schematic of Annuli Investigated by Kjellstrom & Hedberg[8] and Feurstein & Rampf[20].

in Fig. 6) the basic idea proposed by Hall is the following: velocity distributions can be experimentally determined, and from this the point of maximum velocity can be obtained. At this point the velocity gradient, du/dr , equals zero. This is assumed to coincide with the point of zero shear stress, which is true for laminar flow, but not quite true for turbulent flow. In turbulent flow the transport of momentum over short distances via eddies may displace these points by a small amount. This surface of zero shear divides the annulus into two separate flow zones which may be analyzed separately. By applying a force balance on each zone, the drag associated with each surface may be calculated and hence the corresponding friction factor.

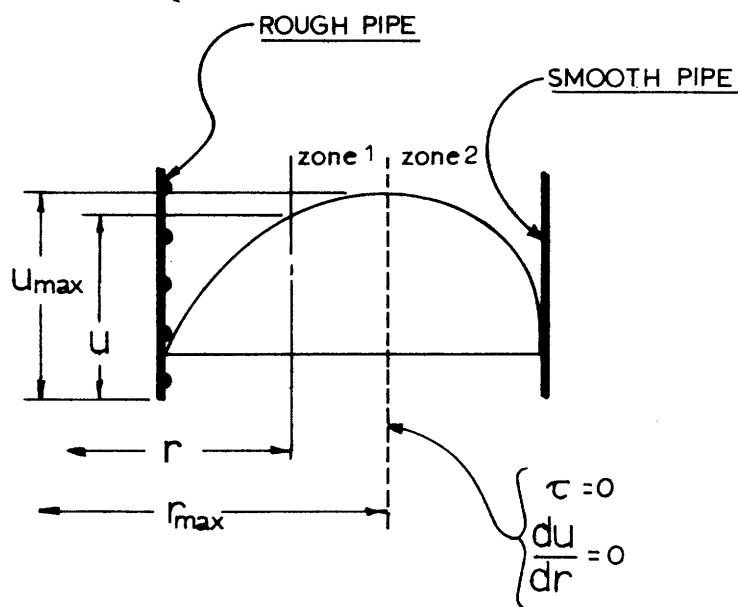


Figure 6. Schematic of Velocity Distribution in an Annular Type Geometry with Inner Surface Rough and Outer Surface Smooth

The assumption of the coincidence of the point of zero shear and the point of zero velocity gradient has been the subject of much experimental investigation [3, 4, 5, 6, 7, 8]. It is now generally accepted that the error introduced by this assumption is small, being less than 10%. An assumption which is made to simplify the calculations is that the density and viscosity of each zone are equal. This is strictly true for an isothermal case. In the present pipe-type case, the temperature gradient between the outside of the cable and the bulk temperature of the fluid is not great enough to cause an appreciable difference between these variables [3]. Another important assumption is that the pressure drop, dp/dx , at any given cross section of pipe is a constant, i.e., $(dp/dx)_1 = (dp/dx)_2 = \dots (dp/dx)_T$. This implies that we have one-dimensional flow throughout the pipe. One of the big disadvantages of the Hall Transformation is that the velocity distributions have to be known to determine the point of maximum velocity. This problem may be circumvented by assuming that the average bulk velocity of the fluid in each adjoining zone are equal. This assumption is not exactly true. However, it has been shown by Wilkie [4, 6] that the average velocity of the outer smooth zone is at most 2% higher than the inner rough zone. For simplicity we shall assume that they are equal.

CHAPTER III

DERIVATION OF METHOD FOR A SIMPLE ANNULUS

The method which will be used to predict the friction factor for pipe-type case will first be developed for a simple annulus. The reason for this is that most of the experimental results in the literature has been performed on annuli, so we have a means to check our theory. The basic concept used here is the same as that for a pipe-type case but may be easier to understand and more accurately grasped.

Definition of the Problem

As was stated previously, the difficulty which exists in the calculation of the pressure drop is from the helically wound semicircular wrappings on the cables. To better understand the problems at hand, one should now refer to figure 7 which was obtained from experimental results on a scale model of a pipe-type cable system for various different cable configurations in the Heat Transfer Laboratory of M.I.T. One of the most striking observations is that turbulent flow seems to exist for a Reynolds number as low as 500. Furthermore, there is no discontinuity which separates laminar from turbulent flow. This is attributed to the fact that the semi-circular wrappings on the cables introduce instabilities into the boundary layer [16]. Also noteworthy is that the friction factor is essentially independent of cable configuration for Reynolds numbers above 2000. Our problem of friction factor prediction may now be divided up into three parts:

1. To find a friction correlation for a surface containing semi-circular, helically wound wrappings.
2. From our knowledge of smooth pipe friction factors to obtain a

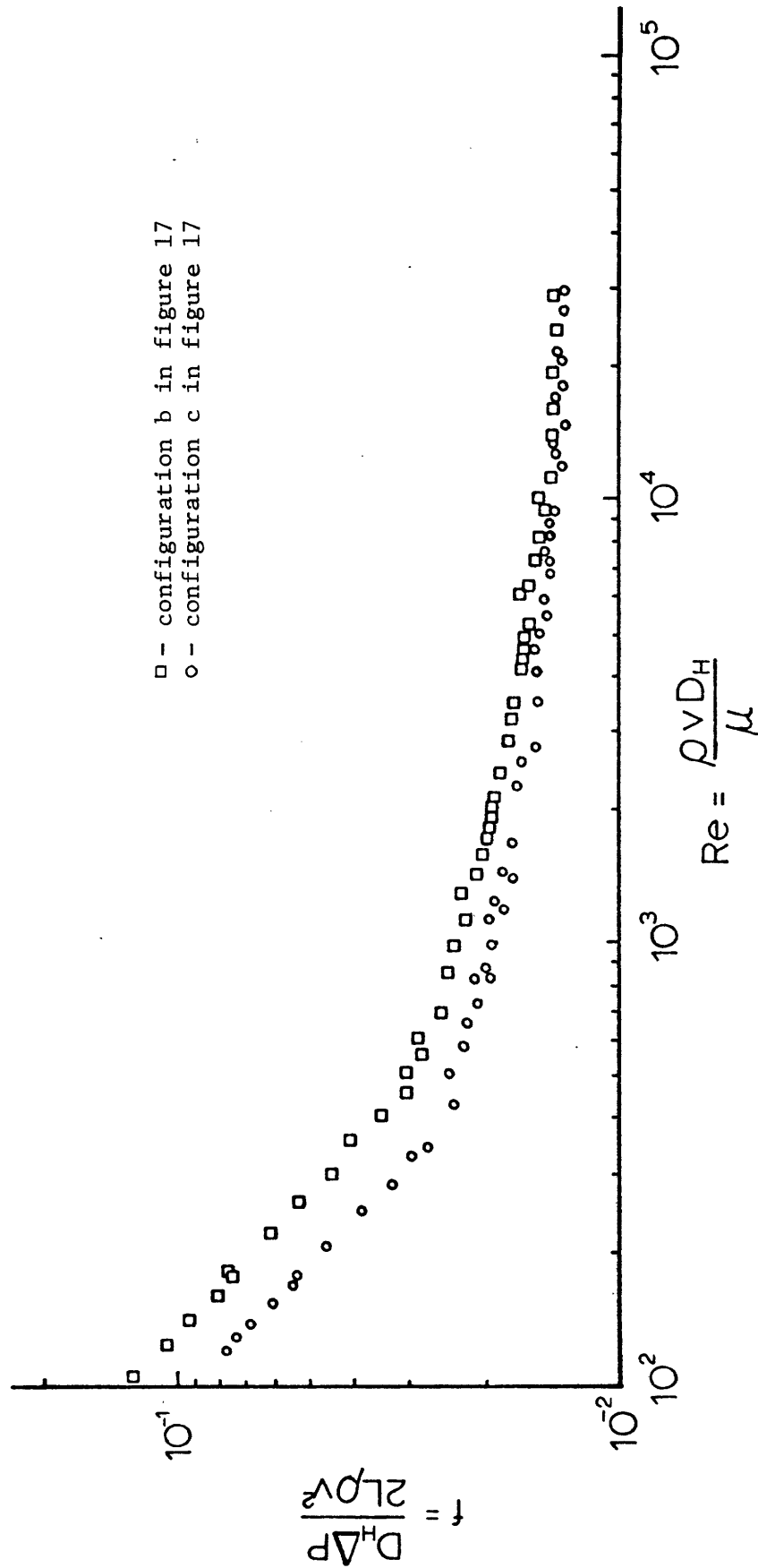


Figure 7. Experimentally Determined Values of Friction Factor vs. Reynolds Number for a Pipe-Type Cable System[1].

correlation which we could use for turbulent flow for a Reynolds number as low as 500.

3. To obtain a method that combines the correlations obtained from parts 1 and 2 in order to obtain a friction factor vs. Reynolds number curve for the entire pipe-type cable geometry.

Each part will be dealt with separately in the following sections.

Friction Factor Correlation for the Rough Surface (Cables)

Unfortunately there does not currently exist a correlation which will predict the friction factor for a rod with semi-circular helically wound cable around it. We must therefore compromise. Eckert et al. [17] has obtained a correlation which will predict the friction factor for flow in a tube with rectangular, transverse ribs machined on the inside wall, similar to the schematic shown in figure 2, as a function of e/D_{HI} and p/e and has verified it for the following ranges:

$$0.01 < e/D_{HI} < 0.04, \quad 0.71 < Pr < 37.6$$

$$10 < p/e < 40 \quad e^+ = \frac{e}{D_c} Re \sqrt{\frac{f}{2}} > 35$$

$$f_i = \frac{2}{\left[2.5 \ln \left(\frac{D_{HI}}{2e} \right) - 3.75 + 0.95 \left(\frac{p}{e} \right)^{.53} \right]^2} \quad (1.)$$

If we could modify this to account for the rounding of the ribs and the varying helix angle, we would have a useful correlation. One of the results obtained from the vast amount of research conducted and collected by D. Wilkie [3] is that chamfering the corners of very sharp rectangular ribs will decrease the friction factor by as much as 8%. It was also found that continued chamfering (such as to obtain a semi-circular shape)

will not have any more of an effect on the friction factor beyond this 8% reduction.

It should be mentioned that these results were obtained for high turbulent Reynolds numbers ($>10^4$). In this regime the boundary layer is quite small relative to the skid wire height. At lower turbulent Reynolds numbers the boundary layer is larger, and the effect of rib profile may have more of an influence on the flow. However, due to lack of any more existing information, we will assume these results to hold equally well at low turbulent Reynolds numbers.

Other experimental results found by Wilkie [3,4] have shown that varying the helix angle of helically wound square ribs will effect the friction factor as shown in figure 8 for pitch to height ratios, p/e , of 8 and 16. These results were also obtained for high turbulent Reynolds numbers which will assume to be valid at low turbulent Reynolds numbers. The effect of rib rounding and varying helix angle are combined and shown as an overall correlation to equation (1) in figure 9. The final correlation to be used in the prediction of the friction factor for the rough surface is,

$$f_i = \frac{2 K(\alpha)}{\left[2.5 \ln\left(\frac{D_H}{2e}\right) - 3.75 + 0.95\left(\frac{p}{e}\right)^{0.53} \right]^2} \quad (2.)$$

where K is a function of the helix angle α , obtained from figure 9. It is now obvious that we have reached a point where we have a lack of information for accurate design purposes. We know that our correction coefficient K is a function of the helix angle (α) and that we should have a family of curves for various p/e ratios. Since only two curves

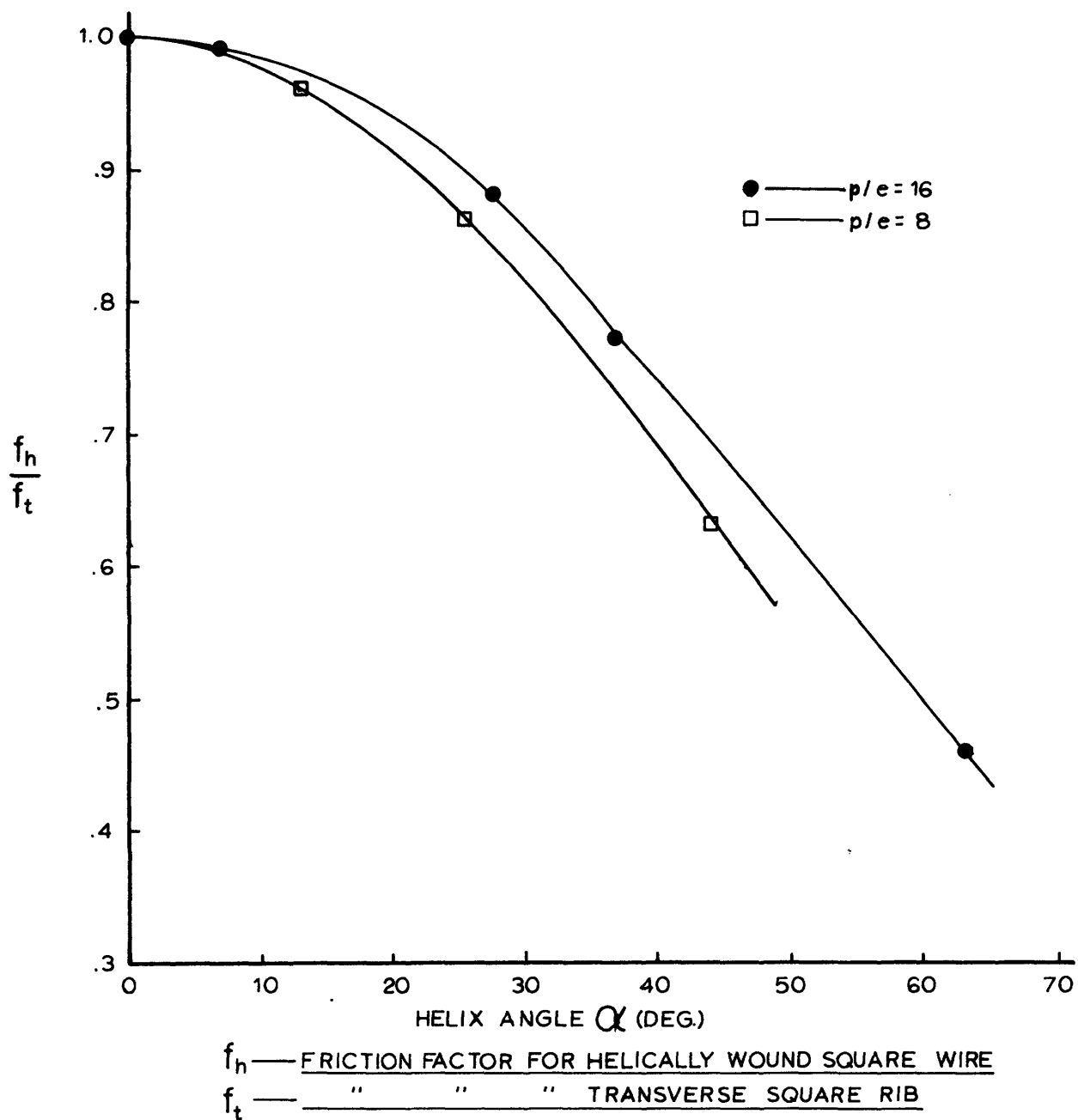


Figure 8. Ratio of Friction Factor for a Helically Wound Square Wire to Friction Factor for a Transverse Square Rib vs. Helix Angle α , from Wilkie[4]

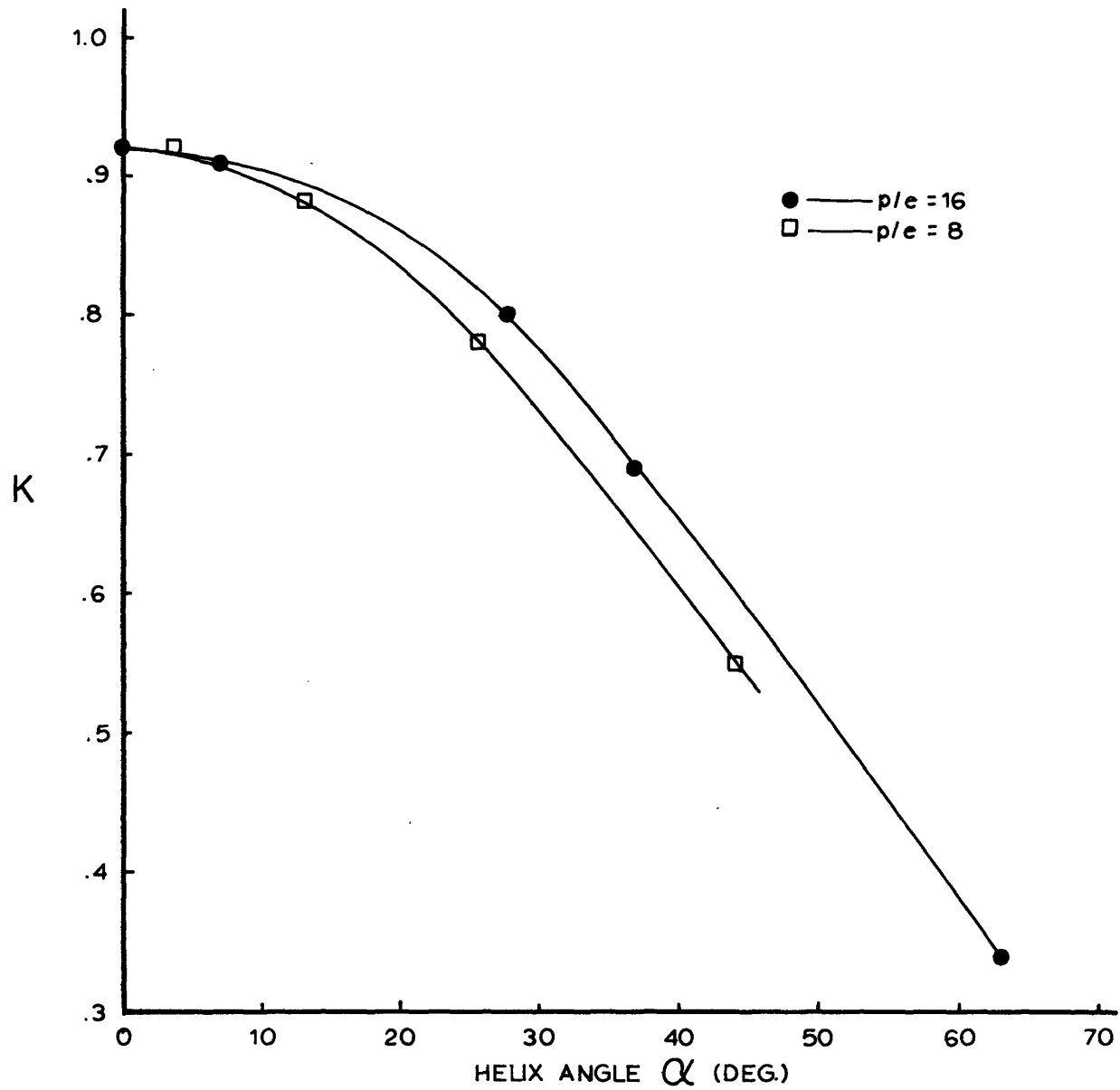


Figure 9. Ratio of Friction Factor for a Helically Wound Circular Wire to Friction Factor for a Transverse Square Rib vs. Helix Angle α , from Wilkie[3,4]

are available ($p/e = 8$, $p/e = 16$), any attempt to design outside of this range is an "engineering approximation", and the results obtained should be weighted accordingly. It should be noted that the variation between these two curves below helix angles of 25° is very small (less than 3%) and that the largest deviation is only 5%, so that one would not expect to introduce much appreciable error by carefully extrapolating outside this range.

Eckert states that his correlation equ. (1) is valid for a roughness Reynolds number e^+ ($e^+ = \frac{e}{D} \text{Re} \sqrt{f/2}$) which is greater than 35. Below this value, he states that it could be modified to yield a slightly more complex equation. This was initially done, but the results did not agree well with experiment; the predicted values being much too low at low Reynolds numbers. It is questionable whether this equation has to be modified at all for low e^+ values, since the data Eckert obtained below this value was sparse and scattered. Equation (1) was used at all e^+ values and yielded good results.

Friction Factor Correlation for the Smooth Surface (Pipe)

The friction factor for a smooth pipe is a well known function of Reynolds number shown on the Moody Diagram of figure 10 [18]. In the laminar range, the relationship between friction factor and Reynolds number may be found analytically as,

$$f_2 = 16/\text{Re}_2 \quad (3)$$

The curve in the turbulent range may be approximated by the following two well accepted correlations [24],

$$f = 0.0791/\text{Re}_2^{0.25} \quad (4)$$

$$f_2 = 0.046/\text{Re}_2^{0.2} \quad (5)$$

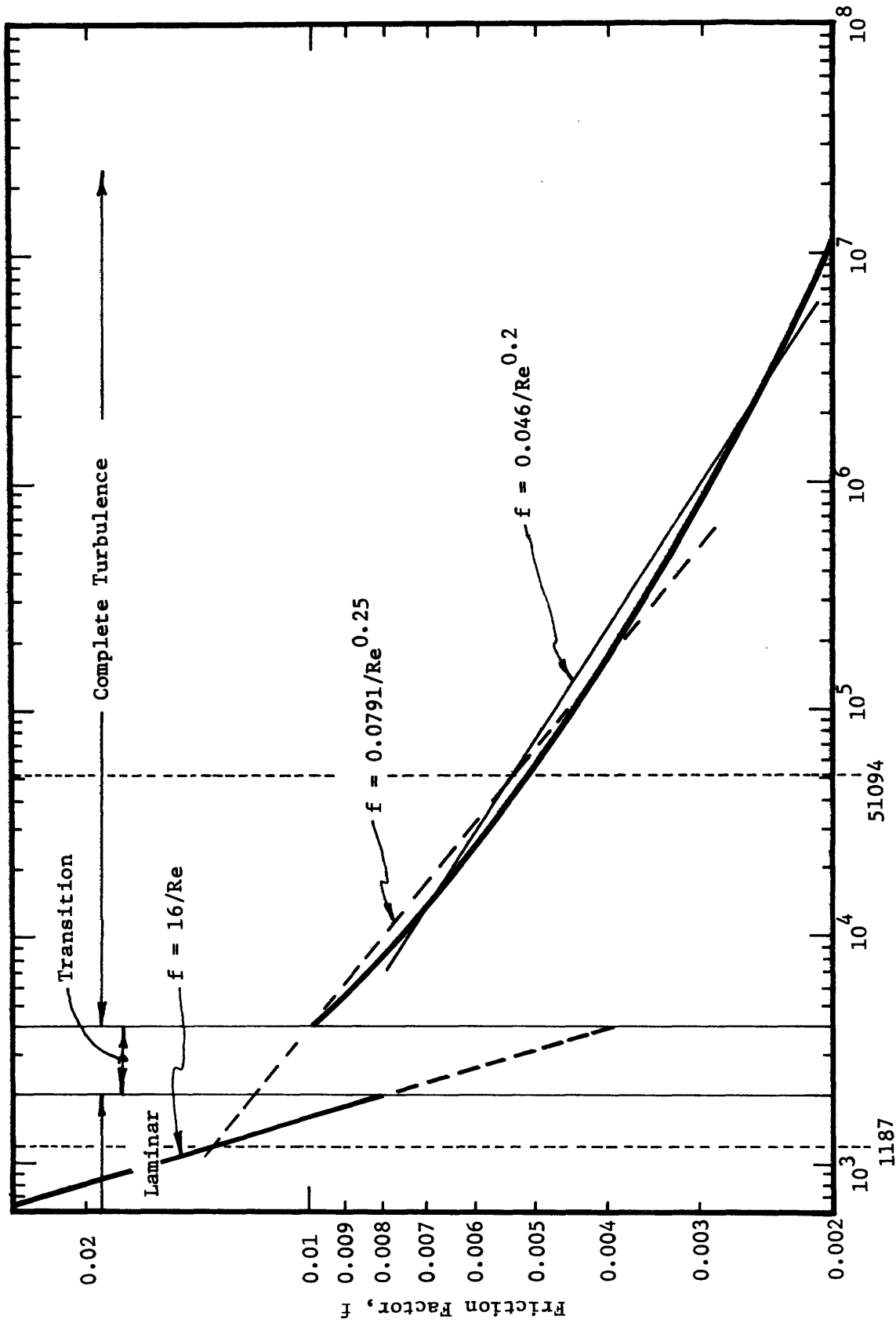


Figure 10. Friction Factor vs. Reynolds Number for a smooth, circular, empty pipe. Moody.[18].

The Reynolds number range in which each applies must be specified. This is discussed below.

In the transition region ($2000 < Re < 4000$) the curve is indeterminate and discontinuous. The flow could either be laminar or turbulent depending on the nature of the flow situation. Laminar flow has been achieved for Reynolds numbers as high as 40,000 [19] by being very careful not to create any outside disturbances in the flow. For a smooth empty pipe, there is a well accepted lower limit of Reynolds number (2000) for turbulent flow, below which the flow will be laminar regardless of any outside disturbances which may be introduced. It should be emphasized that the previous limits on Reynolds numbers have been subject to "external" constraints. We should now remember that we do not have a fully empty smooth pipe. There exist cables in the pipe with turbulence promoters (skid wires). It has been found that turbulence promoters similar to the type considered here are able to reduce the lower limit of Reynolds number (based on the height of the roughness element) at which turbulent flow may exist to approximately 600 [16]. For our pipe-type case, the lower limit of Reynolds number based on the hydraulic diameter has been found experimentally to be approximately 500 (figure 7). We also do not have any discontinuity at the transition point. It would therefore seem reasonable to modify our smooth pipe friction correlations so that there does not exist any discontinuities. This is what was done. Equation (3) was found to intersect equation (4) at a Reynolds number of 1187 for the same friction factor. Similarly, equation (4) intersects equation (5) at a Reynolds number of 51,094. Our final continuous correlation for the smooth pipe friction factor is as follows:

$$f_2 = \begin{cases} 16/Re_2 & Re < 1187 & (6a) \\ 0.0791/Re_2^{0.25} & 1187 < Re < 51094 & (6b) \\ 0.046/Re_2^{0.2} & Re > 51094 & (6c) \end{cases}$$

It should be noticed that we will be using a value of friction factor obtained from laminar flow theory when we actually do not have laminar flow. However, if equation (6b) was used below a Reynolds number of 1187, the friction factor would be less than the laminar value predicted by equation (6a). If the flow is turbulent, it should be expected that the friction factor is at least as large as the laminar value. For lack of any better information, equation (6a) is used for the range indicated.

The author initially assumed equation (4) to hold for low value of Re_2 with the idea that using a value predicted for f_2 from laminar theory in turbulent flow would not be acceptable. The predicted values obtained from using this equation did not possess the slope characteristic of the experimental values in figure 7 in the Reynolds number range 500 - 2000. It was then thought to use equation (3) for low values of Re_2 , purely in the mathematical sense as yielding a value of f_2 for a given Re_2 without any connotations of being either laminar or turbulent. The results obtained by doing this yields the desired slope.

Combination of Smooth and Rough Surface Friction Correlations to Obtain an Overall Friction Factor vs. Reynolds Number

The basic method used to combine the effects of the rough and smooth surfaces is the Hall Transformation mentioned previously. This assumes that we have a position of zero shear which separates the effects of the rough surface from the smooth. We further assume that in each zone, the

pressure gradient, mean velocity, density, and viscosity are equal. The assumption of equal mean velocities considerably simplifies the analysis and for the test cases does not introduce significant errors.

We begin the development of the method by defining the following variables:

Hydraulic Diameter:

This is defined as being equal to four times the cross sectional area of the flow divided by the wetted perimeter. In an annulus shown schematically in figure 11, the hydraulic diameter of zone 1, D_{H1} , is equal to four times the cross sectional area between the inner rough surfaces and the radius of zero shear ($\gamma = 0$) divided by the perimeter of the inner rough surface, i.e.,

$$D_{H1} = \frac{4A_1}{C_1}$$

It should be noted that the perimeter along the zero shear boundary is not included in the wetted perimeter.

Similarly, $D_{H2} = 4A_2/C_2$, where A_2 is the area between the radius of zero shear and the smooth surface and C_2 is the circumference of the outer smooth pipe.

Following the same reasoning, D_{H12} , the hydraulic diameter of the entire annuli is defined as follows:

$$D_{H12} = \frac{4(A_1 + A_2)}{(C_1 + C_2)} = \frac{4A_{12}}{(C_1 + C_2)}$$

Friction Factor:

$$f = \left(\frac{dp}{dx}\right) \frac{D_H}{2\rho V^2}$$

Reynolds Number:

$$Re = \frac{V D_H}{\nu}$$

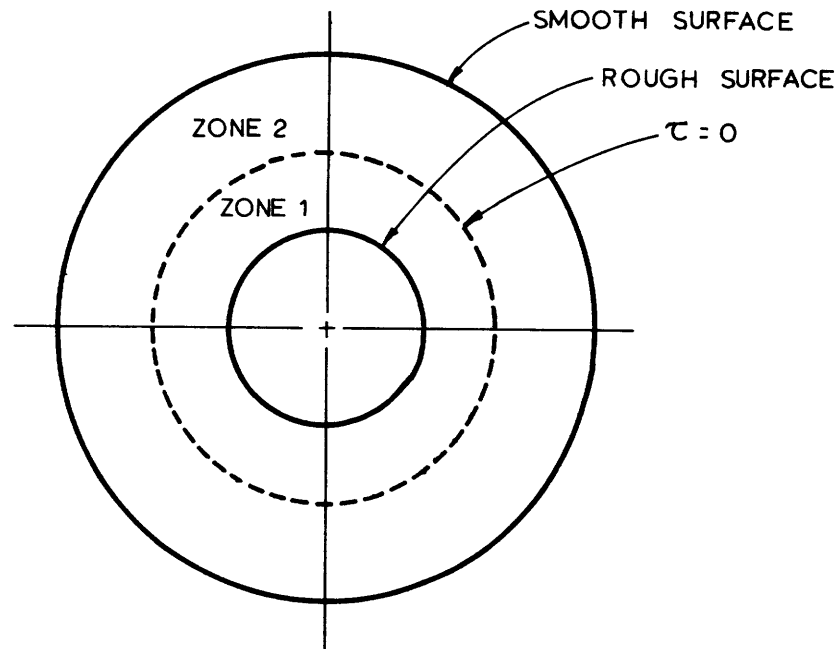


Figure 11. Cross Section of Annular Type Geometry

From the assumption that the pressure gradient in each sub-channel are equal, we may write,

$$\left(\frac{dp}{dx}\right)_1 = \left(\frac{dp}{dx}\right)_2 \quad (8)$$

or

$$\frac{2f_1 \rho_1 V_1^2}{D_{H1}} = \frac{2f_2 \rho_2 V_2^2}{D_{H1}} \quad (9)$$

Since

$$\rho_1 = \rho_2, v_1 = v_2, \text{ we have,}$$

$$\frac{f_1}{D_{H1}} = \frac{f_2}{D_{H2}} \quad (10)$$

To find a relationship between D_{H1} and D_{H2} , we make use of the following identity:

$$\frac{4A_1}{C_1} + \frac{4A_2}{C_1} = \frac{4(A_1 + A_2)}{C_1} \quad (11)$$

Now, recalling the definition of hydraulic diameter as four times the cross sectional area divided by the wetted perimeter ($D = \frac{4A}{C}$), this reduces to

$$D_{H1} + \frac{C_2}{C_1} D_{H2} = \frac{C_1 + C_2}{C_1} D_{H12} \quad (12)$$

It should be realized that the following relation holds since it was assumed that the mean velocities, densities, and viscosities are equal on both sides of the zero shear plane.

$$Re_2 = \frac{D_{H2}}{D_{H12}} Re_{12} \quad (13)$$

where Re_2 is the Reynolds number for zone 2 and Re_{12} is the Reynolds number for the combined zones 1 and 2 (in this case, $Re_{12} = Re_T$, where Re_T is the Reynolds number of the entire geometry).

We now have five equations (2,6,10,12,13) and six unknowns ($f_1, f_2, D_{H1}, D_{H2}, Re_2, Re_{12}$). We could pick a value for one of them and solve

for the rest, which is what the computer program does. It picks a value D_{H1} and solves for Re_{12} . D_{H1} was chosen as the independent variable since it has definite limits which are easily found. The lower limit on D_{H1} is zero, which occurs at low Reynolds numbers when most of the flow is influenced by the smooth pipe friction correlation. The upper limit on D_{H1} occurs at very large Reynolds numbers when the flow is completely turbulent and influenced chiefly by the rough surface. This upper limit is: $D_{H1}(u1) = 4A_{12}/C_1$.

To obtain the corresponding overall friction factor, f_{12} , (in this case, $f_T = f_{12}$) the same procedure is followed as before, only this time requiring that the pressure drop of the total passage to be the same as each sub-channel.

$$\left(\frac{dp}{dx}\right)_{12} = \left(\frac{dp}{dx}\right)_1 \quad (14)$$

which reduces to,

$$\frac{f_{12}}{D_{12}} = \frac{f_1}{D_1} \quad (15)$$

By using the same independent value of D_{H1} that was used to obtain Re_{12} , we can solve equations (2) and (15) simultaneously to obtain the friction factor f_{12} for the corresponding Reynolds number Re_{12} .

CHAPTER IVCOMPARISON OF THEORY WITH EXPERIMENT FOR FLOW INTUBES AND ANNULAR TYPE GEOMETRIES

There have been numerous experiments performed which enable us to test our theory at various stages of its development. We first test it against a tube containing helically wound coils and then with data obtained from experiments performed on concentric annuli type geometries.

Test of Rough Friction Correlation - Equation (2)

Equation (2) should be able to predict the friction factor for a tube with round, helically wound coils pressed tightly against its walls as shown in figure 3. Since the hydraulic diameter in this case is constant and equal to the diameter of the pipe, this equation will predict a constant value of friction factor, independent of Reynolds Number. E.W. Sams [15] in 1957 determined the friction factors for various size coil diameters and pitches for a similar type geometry. Figure 12 shows his experimentally determined values and the value of f as predicted from equation (2). The agreement is quite good.

Test of Modified Hall Transformation

An annuli, unlike the tube just described, will not have a constant hydraulic diameter associated with each sub-channel on each side of the line of zero shear stress. Only the hydraulic diameter of the entire annuli will be a constant. The sub-channel hydraulic diameters will be a function of Reynolds Number. At low Reynolds Numbers, one would expect the line of zero shear to be closer to the inner rough surface. This will increase the area associated with the smooth surface friction factor and

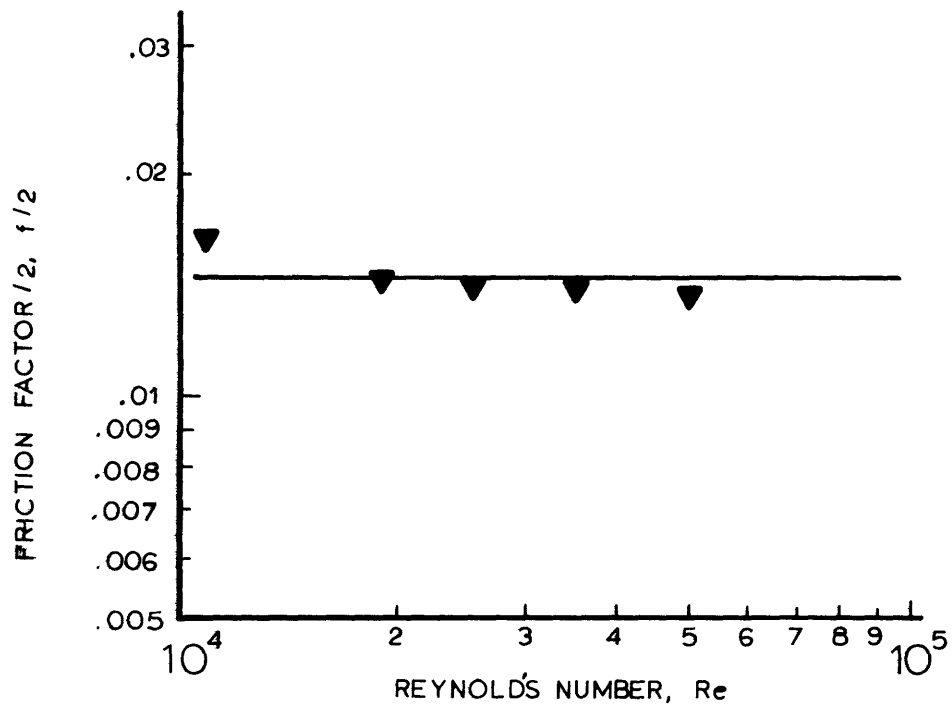


Figure 12. Comparison of Experimental Data Obtained From a Roughened Tube Similar to the One Shown in Figure 3 with Theoretically Predicted Values. Data is from Sams[15].

increase its influence in the friction factor for the entire annuli. Conversely, at high Reynolds numbers, one would expect the flow to be influenced chiefly by the effects of the rough surfaces. This means that the zero shear line will move closer to the outer smooth surface thereby increasing the hydraulic diameter of the rough surface. The important point is to realize the important effect the Reynolds number has on the hydraulic diameters of the sub-channels, the entire annuli, and consequently the appropriate friction factor.

Sherriff & Gumley [9] in 1966 performed an experiment to determine the friction factor for the rough surface on a concentric annuli with the inner surface roughened with helically wound circular wires at a negligible helix angle and the outer surface smooth (fig. 4). They experimentally determined the velocity profiles and hence the position of zero shear, and were thus able to calculate the friction factor for the rough surface as a function of Reynolds number. Their results are shown in figure 13 along with the values predicted from our theory.

Kjellstrom & Hedberg [8] in 1966 performed an experiment to determine the friction factor for a concentric annuli with the inner surface composed of rectangular transverse ribs and the outer surface smooth (figure 5). Since the rough surface is composed of rectangular, transverse ribs, there is not only any need to modify Eckerts correlation and we should use equ. (1) instead of (2) in our theory. Remember, the distinction between these two equations is that equ. (1) is for a rough surface composed of rectangular, transverse ribs and that equ. (2) is for a rough surface composed of helically wound cables, which may be either of a square type or round cross section. If it is square, figure 8 should be used to obtain $K(\infty)$, and if it is round, figure 9 should be used to obtain $K(\infty)$. The comparison

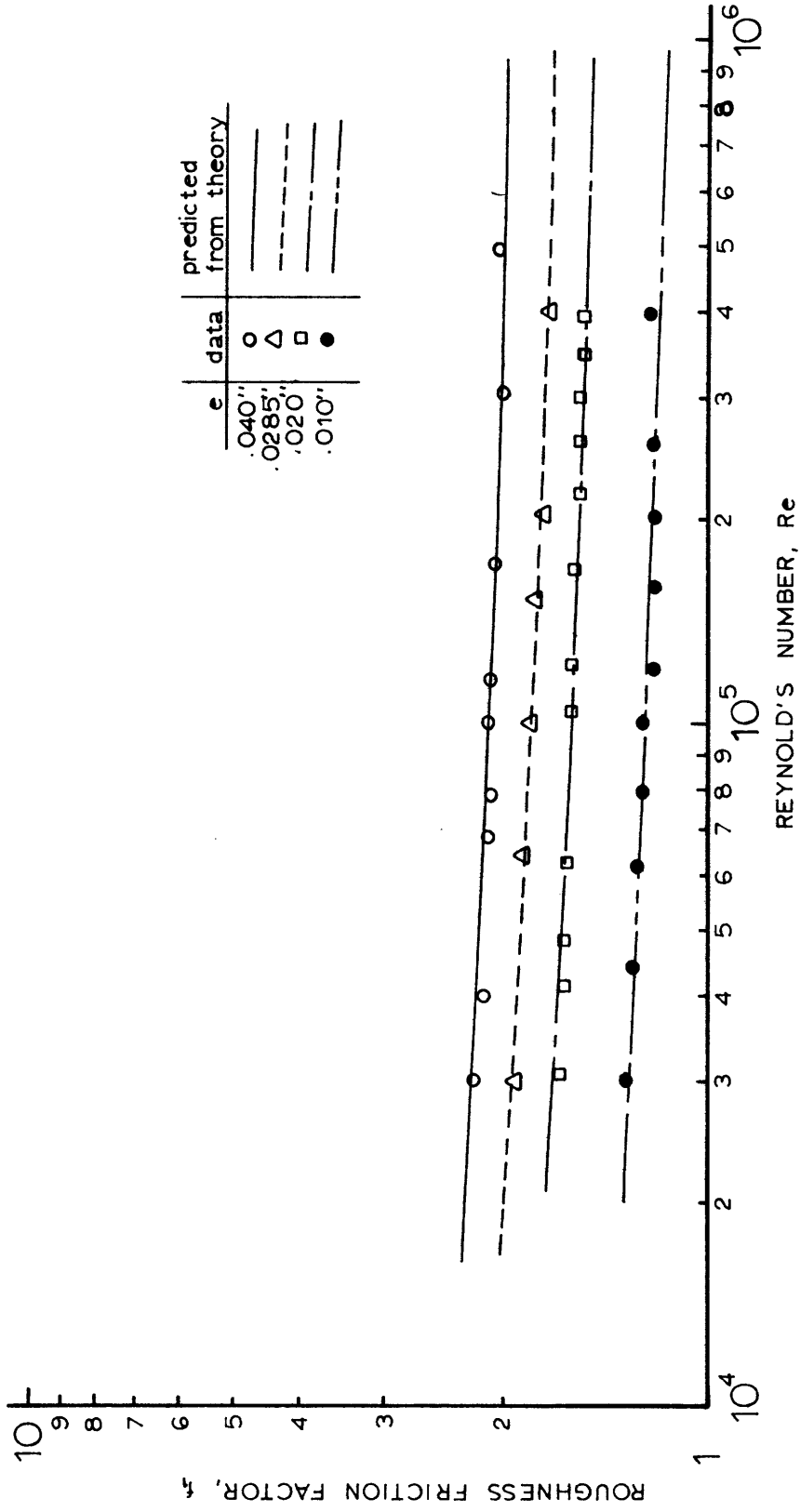


Figure 13. Comparison of Predicted Values of Roughness Friction Factor with Experimental Data for a Concentric Annuli Similar to the One Shown in Figure 9. Data is from Sheriff & Gumley[9].

between the experimental results and our theory is shown in figure 14. It should be noticed that the p/e ratio of the rough surface is 8.62. This is outside of the range of p/e values for which Eckert's correlation has been tested for and could help to explain the 20% error in the prediction.

The last test of our theory is from data obtained from Feurstein & Rampf [20] in 1969 on a concentric annuli similar to the one just mentioned, (fig. 8). In these experiments, the p/e ratios ranged from 10-30; therefore, we should expect better results. The experimental results and theoretically predicted values are shown plotted in figures 15 and 16. The comparison is quite good.

The comparisons of the predictions of Eckert's modified correlations, equation (2), with experimental data (figures 12 & 13) is very good. The predictions of the total friction factor for an annuli are consistently below the experimentally determined values (figures 14, 15, & 16). Therefore, there seems to be some error introduced by the use of our modified Hall Transformation; the exact cause of which is unknown by the author. More will be said about this at the end of Chapter VI.

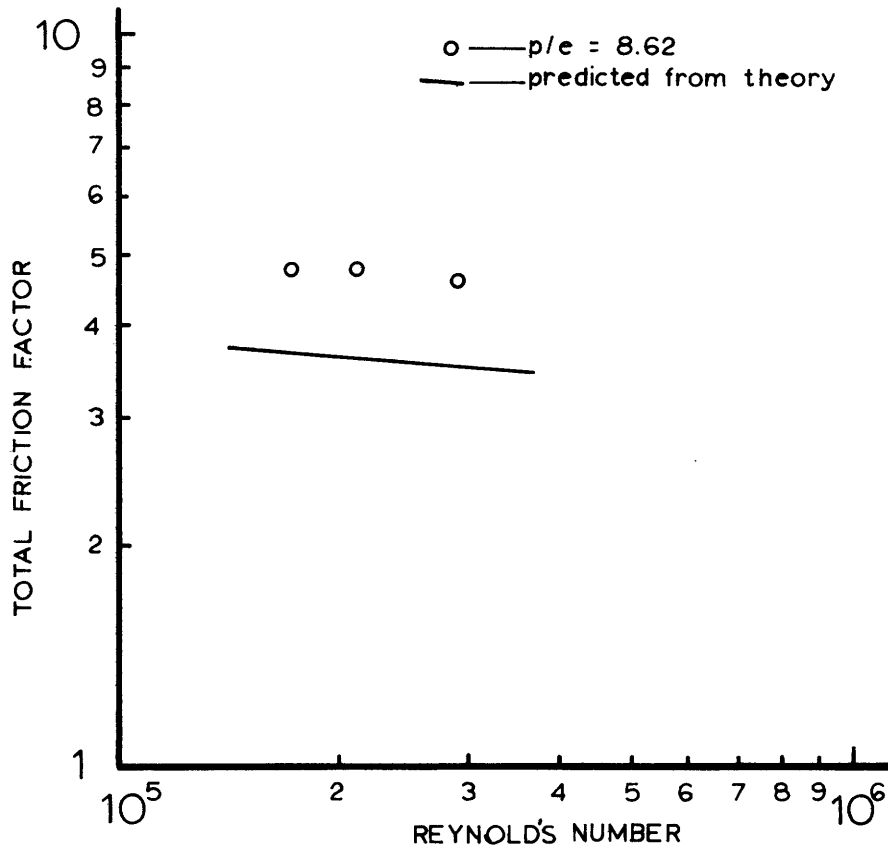


Figure 14. Comparison of Predicted Values of Total Friction Factor with Experimental Data for a Concentric Annuli Similar to the one Shown in Figure 10. Data is from Kjellstrom & Hedberg[8].

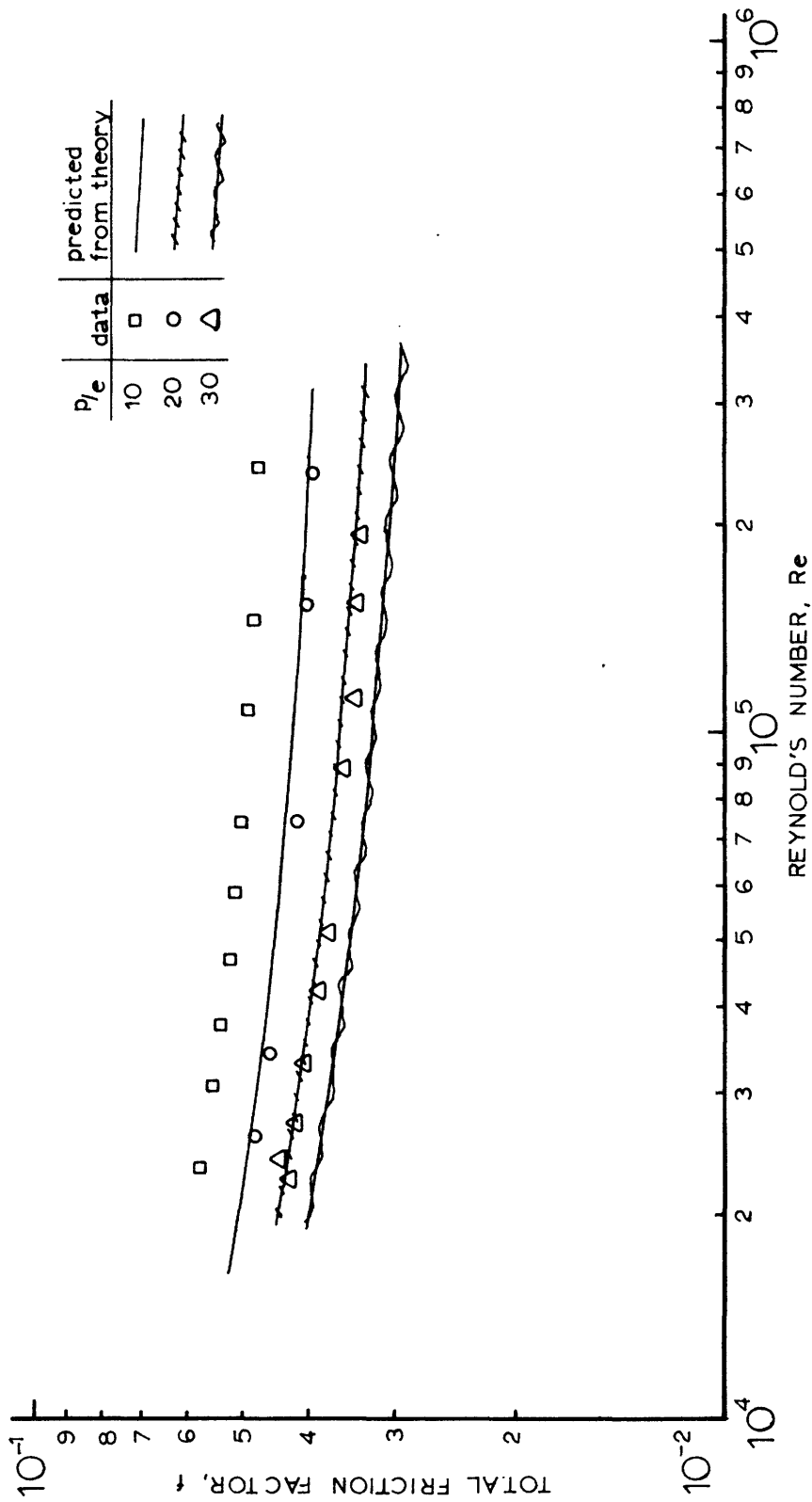


Figure 15. Comparison of Predicted Values of Total Friction Factor with Experimental Data for a Concentric Annuli Similar to the one Shown in Figure 5. Data is from Feurstein & Rampf[20]. ($e=4$ mm.)

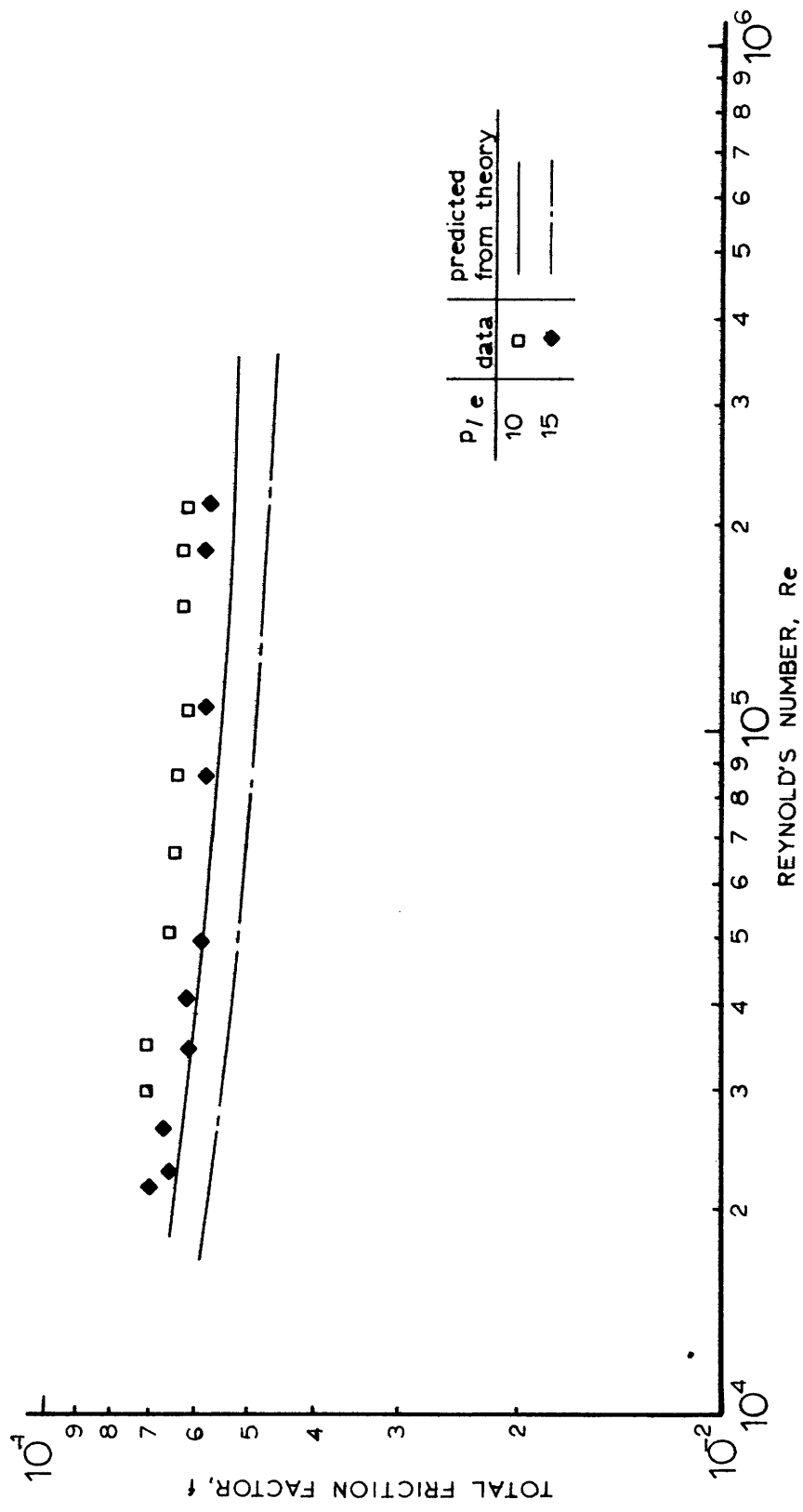


Figure 16. Comparison of Predicted Values of Total Friction Factor with Experimental Data for a Concentric Annuli Similar to the one Shown in Figure 5. Data is from Feurstein & Rampf[20]. (e=2 mm.)

CHAPTER VEXTENSION OF METHOD FROM ANNULAR TO PIPE-TYPE CASE

The extension of the theory from the annular case to the pipe-type case in which there exist three cables in a smooth conduit is simple and straightforward. Four cable configurations were chosen to be modelled (figure 17). In each case, the flow area is broken up into separate flow zones, the boundaries being the assumed ones of zero shear.

Configuration a is the easiest to analyze. In this configuration, all three cables are assumed to be touching one another grouped in the center of the conduit. The flow area between the cables is small and is neglected, as is the circumference of the cables bordering this area. We are left with a modified annular type geometry. The flow area is equal to the area of the pipe minus the combined areas of the cables plus the neglected trapped area. The wetted perimeter of zone 1 is equal to the combined circumference of the cables minus the portion that borders the trapped center region. By making these simple assumptions with regard to areas and circumferences, the pipe-type cable case is transformed into an annular type case, and the equations of Chapter III apply directly.

We now move to the cable configuration in which there exist three flow zones (configuration b). In this case, the center region (3) between the three cables is not neglected and is considered in the analysis. It is assumed that the flow in this region is influenced solely by the three cables. Its area and circumference are constant; therefore, its hydraulic diameter is constant. With a constant hydraulic diameter equation (2), which predicts the friction factor for the rough geometry, will yield a

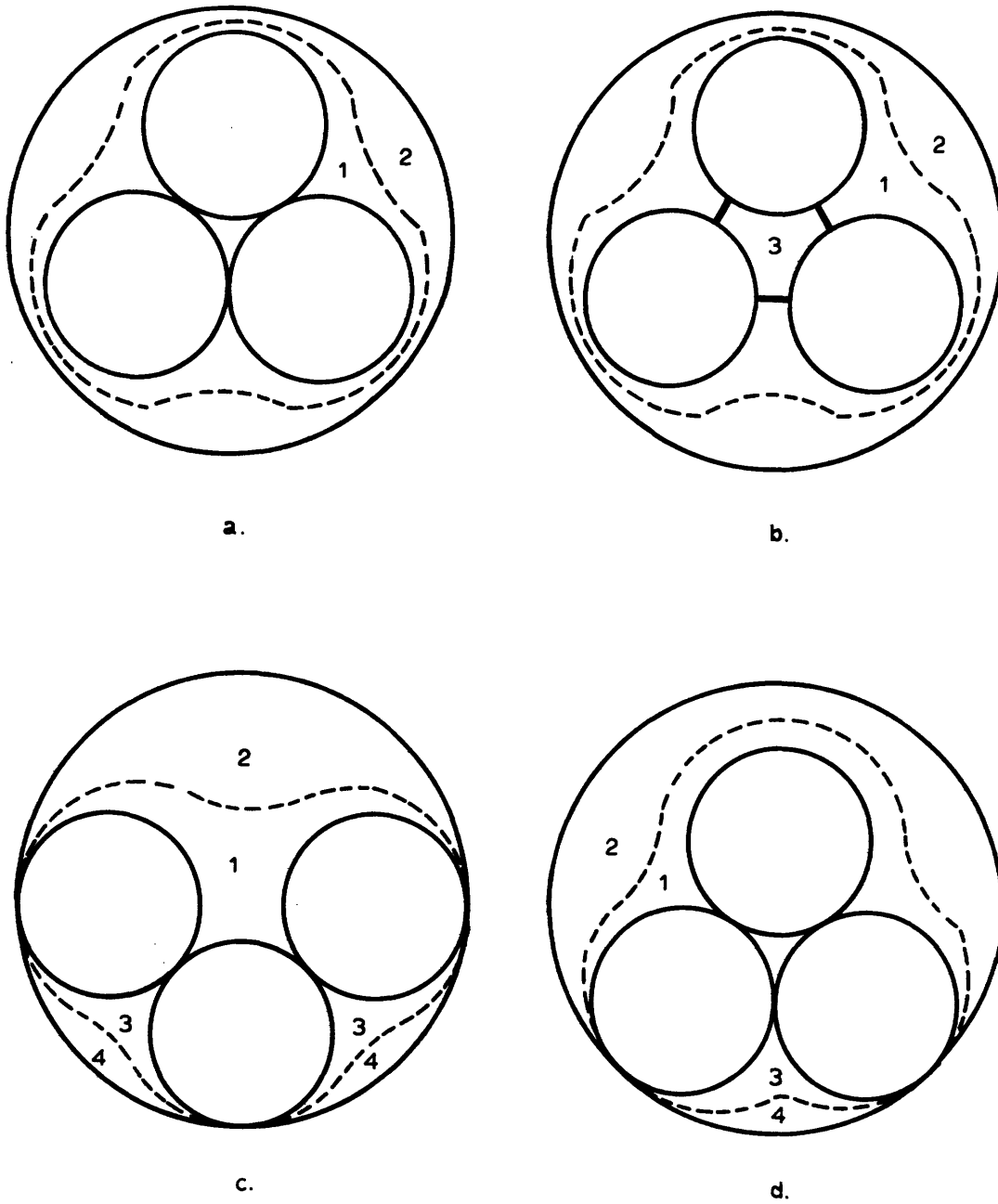


Figure 17. Various Pipe-Type Configurations Modelled Shown Divided into Theoretical Flow Zones (dashed lines).

constant value for f_3 . Zones 1 and 2 are assumed to interact and are treated just like the annular case in Chapter III. We now have a friction factor relationship for the combined zone 12 and a constant value of friction factor, f_3 , for zone 3. Since we want the total friction factor, f_T , we apply our assumption that the pressure drop at any given cross section of pipe is constant. Stated mathematically, this is,

$$\left(\frac{dp}{dx}\right)_T = \left(\frac{dp}{dx}\right)_{12} \quad (16)$$

which says that the pressure drop of the total pipe-type system is the same as the pressure drop in the combined zone 12. This may also be expressed as,

$$\frac{2f_T \rho_T \bar{V}_T^2}{D_{HT}} = \frac{2f_{12} \rho_{12} \bar{V}_{12}^2}{D_{12}} \quad (17)$$

which reduces to,

$$f_T = \left(\frac{D_{HT}}{D_{12}}\right) \left(\frac{\bar{V}_T^2}{\bar{V}_{12}^2}\right) f_{12} \quad (18)$$

It should be noted that in this case, we are not assuming that the mean velocity of zone 3 is equal to zone 12. We are separating zone 3 from zone 1 by an imaginary boundary. The flow in zone 3 is not assumed to be influenced by zone 1, therefore the mean velocity of zone 3, \bar{V}_3 , is not equal to the mean velocity of zone 1, \bar{V}_1 . Consequently, $\bar{V}_3 \neq \bar{V}_T$ and $\bar{V}_{12} \neq \bar{V}_T$. We must somehow find a relation between the mean velocities \bar{V}_{12} and \bar{V}_T . This is accomplished by making use of the fact that the mass flow at any given cross section is a constant.

$$\dot{m}_T = \dot{m}_{12} + \dot{m}_3 \quad (19)$$

which may be expressed as,

$$\rho_T A_T \bar{V}_T = \rho_{12} A_{12} \bar{V}_{12} + \rho_3 A_3 \bar{V}_3 \quad (20)$$

Since the density is assumed constant, this reduces to

$$A_T \bar{V}_T = A_{12} \bar{V}_{12} + A_3 \bar{V}_3 \quad (21)$$

Upon rearranging, we have,

$$\frac{\bar{V}_T}{\bar{V}_{12}} = \frac{1}{A_T} \left[A_{12} + \frac{Re_3}{Re_{12}} \frac{D_{H12}}{D_{H3}} A_3 \right] \quad (22)$$

We have now found our desired relation, but in doing so, have introduced another unknown, the Reynolds number for zone 3, Re_3 . This is taken care of by applying our assumption of constant pressure drop at any cross section of pipe. This time, we consider the combined region 12 and region 3.

$$\left(\frac{dp}{dx} \right)_{12} = \left(\frac{dp}{dx} \right)_3 \quad (23)$$

or equivalently,

$$\frac{f_{12} \bar{V}_{12}^2}{D_{H12}} = \frac{f_3 \bar{V}_3^2}{D_{H3}} \quad (24)$$

which may be expressed as:

$$\frac{f_{12}^{0.5} Re_{12}}{D_{H12}^{1.5}} = \frac{f_3^{0.5} Re_3}{D_{H3}^{1.5}} \quad (25)$$

Solving for Re_3 , we have:

$$Re_3 = \frac{D_{H3}}{D_{H12}} \frac{f_{12}}{f_3} Re_{12} \quad (26)$$

The overall Reynolds number, Re_T , is obtained by making use of the following identity:

$$Re_T = \frac{D_{HT}}{D_{H12}} \frac{\bar{V}_T}{\bar{V}_{12}} Re_{12} \quad (27)$$

Summarizing, for a cable configuration which we divide into three zones, the third of which is considered independent of the other two, we proceed as follows:

1. Solve for the friction factor-Reynolds number relationship for zone 12 as outlined in Chapter III.
2. Calculate the constant friction factor for zone 3.
3. Solve for the overall friction factor-Reynolds number relationship by using equations (18), (22), (26), and (27).

It should now be obvious that we could handle configurations c & d in the same manner that we treated configuration b, simply by replacing zone 3 by the combined zone 34.

However, the friction factor for zone 3 in configuration b was a constant. This is not so for zone 34 for configurations c & d. It is clearly a function of Reynolds number just like region 12. We must therefore

use some ingenuity in obtaining the overall friction factor, We first obtain a relationship f_{12} vs. Re_{12} and f_{34} vs. Re_{34} by the method outlined in Chapter III. The fact that we do not have anything that resembles an annular type geometry does not make any difference, since the hydraulic diameter effectively accounts for this. We then use the same reasoning as before to obtain equations (16), (17), & (18). The conservation of mass equation becomes:

$$\dot{m}_T = \dot{m}_{12} + b\dot{m}_{34} \quad (28)$$

where b is a constant and is equal to 1 for configuration d and equal to 2 for configuration c. This equation reduces to

$$A_T \bar{V}_T = A_{12} \bar{V}_{12} + b A_{34} \bar{V}_{34} \quad (29)$$

which, upon rearranging, yields:

$$\frac{\bar{V}_T}{\bar{V}_{12}} = \frac{1}{A_T} \left[A_{12} + b \frac{Re_{34}}{Re_{12}} \frac{D_{H12}}{D_{H34}} A_{34} \right] \quad (30)$$

As before, we have found a relationship for our velocities, but in doing so, we have introduced another variable, this time Re_{34} . If the constant pressure drop criterion is applied as before, we obtain:

$$\frac{dp}{dx_{12}} = \frac{dp}{dx_{34}} \quad (31)$$

or, equivalently,

$$\frac{f_{12} \bar{V}_{12}^2}{D_{H12}} = \frac{f_{34} \bar{V}_{34}^2}{D_{H34}} \quad (32)$$

which may be expressed as,

$$\frac{f_{12}^{0.5} Re_{12}}{D_{H12}^{1.5}} = \frac{f_{34}^{0.5} Re_{34}}{D_{H34}^{1.5}} \quad (33)$$

Equation (33) contains two unknowns, Re_{12} and Re_{34} (f_{12} is a function of Re_{12} and f_{34} is a function of Re_{34}). With configuration b, f_3 (corresponding to this f_{34}) was a constant and the equation could be solved explicitly. In this case, f_{34} is not a constant but is a function of Reynolds number. The procedure which is used in solving this equation is as follows:

1. Assume that each side of the equation as it is written is a single valued function of f_{12} and f_{34} .
2. Pick a value of f_{12} and solve the left hand side for a constant.
3. Since the right hand side is equal to the same constant, proceed to pick various values of f_{34} until this constant is obtained.

Equation (30) may now be solved with equation (18) to obtain the total friction factor, f_T . The corresponding total Reynolds number, R_T , may be found by the use of equation (27).

Summarizing, to obtain the overall friction factor vs. Reynolds for a pipe-cable geometry which is divided into flow zones which are independent of one another and each having a functional relationship between its friction factor and Reynolds number (such as configurations c & d), we proceed as follows:

1. Solve for the friction factor-Reynolds number relationship for the sub zones 12 and 34 as outlined in Chapter III.

2. Solve equation (33) iteratively as outlined to obtain a relationship between Re_{12} and Re_{34} .
3. Use the value obtained in 2 to solve equations (30), (27), and (18), using the appropriate value for b .

CHAPTER VI
COMPARISON OF THEORY WITH EXPERIMENT
FOR FLOW IN A PIPE-TYPE CABLE SYSTEM

Figure 18 shows the comparison of the values of friction factor obtained experimentally at M.I.T.'s Heat Transfer Laboratory and the values predicted by the method described previously. Configurations b & c were the upper and lower bounds found experimentally, which is also predicted for the theory.

The asymptotic friction factor for configuration b is 0.0132, for configuration a is 0.0130, for configuration c is 0.0109, and for configuration d is 0.0095.

The results from the most conservative approximation (configuration b) are consistently 15-30% above the experimentally determined values. It should be mentioned that the predictions of configuration a or b are only approximately 15% above the experimentally determined values in the range $500 < Re < 1000$, increasing to 25% at a Reynolds number of 2000 and to 30% above 3000. Therefore, in the range of interest ($Re \approx 500$), the use of configurations a or b will predict a value of friction factor approximately 15% too high.

It is recommended that the value of the friction factor to be used for design purposes be the average value of the friction factor as predicted from configurations a and c. For the present case, this value would be just about right at low Reynolds numbers, the error increasing to only 22% at a Reynolds number of 10,000.

These errors may be attributed to the method used to combine the

EXPERIMENTAL DATA FOR MODEL FROM [1]

- configuration b
- configuration c

PREDICTED FROM THEORY	CONFIGURATION
---	b
—	a
—	c
—	d

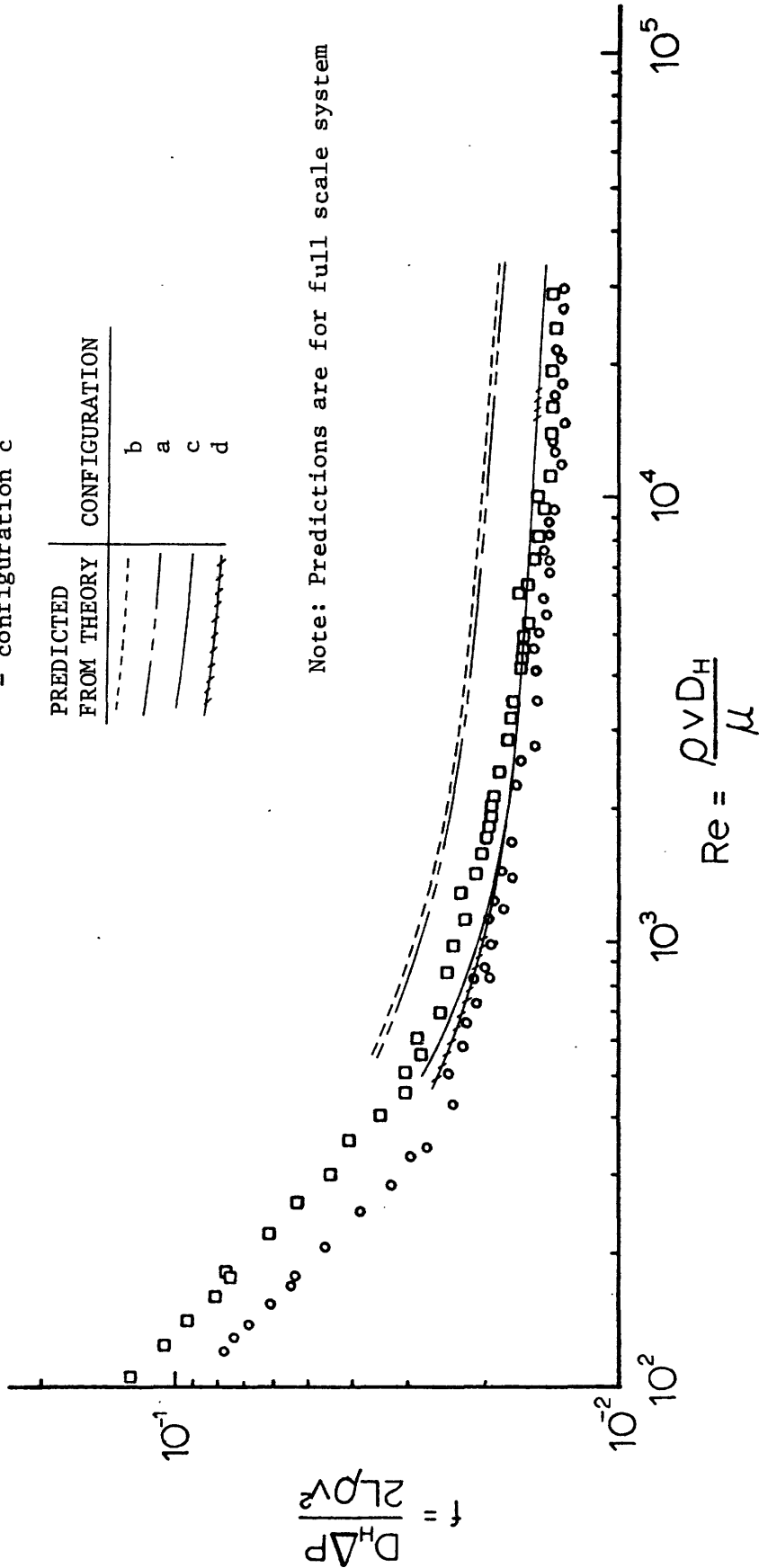


Figure 18. Friction Factor vs. Reynolds Number for Pipe-Type Cable System. Experimental points are for scale model. Predicted values are for full scale system.

rough and smooth surface effects, i.e., the modified Hall Transformation. It does not seem to properly weight each effect as they are combined. In the annular case, where there is only one roughened rod, the theory seems to weight the effects of the smooth surface too much, leading to a predicted value of friction factor which is too low. In the pipe-type case, the rough surface seems to be weighted too much, leading to a predicted value of friction factor which is too high. The actual cause in the imbalance of this weighting process is unknown. The only possible explanation the author has is that the basic assumption of equal pressure drops in each flow zone is not exactly true, i.e., the flow is not completely one dimensional. In the annular case, the rough surface was not large enough to cause sufficient mixing between the two zones whereas in the pipe-type case, there may be a "surplus" of rough geometry which would cause a larger degree of mixing and lead to a higher friction factor.

CHAPTER VIICONSIDERATION OF THE EFFECTS ON THE FLOWWHEN A POINT OF CONTACT OCCURS

A point of contact occurs when two cables or a cable and the pipe touch one another. When this occurs, it is conceivable that the flow near the areas of contact may be laminar. This was assumed to be the case, and an attempt was made to model the system including these laminar zones whenever there is a point of contact. These laminar zones should vanish in the limit as the Reynolds number approaches infinity when the flow is 100% turbulent. As the Reynolds number decreases, these laminar zones should increase, having more of an effect as the Reynolds number is continually decreased. When a laminar zone exists at a point of contact, it is evident by the nature of the geometry that it will contain a relatively small area and large perimeter (figure 19). The existence of these laminar zones means that the turbulent flow region is reduced by an amount equal to the laminar regions. Since the cross sectional area that these laminar zones occupy is relatively small compared to the total flow; whereas, the perimeter that borders these regions is not, the major effect that the laminar zones has on the flow is a decrease in the hydraulic diameter for the turbulent region. This in turn means a reduction in the friction factor at low Reynolds numbers.

The model of the laminar zone for a cable to cable contact did lower the friction factor as predicted but the magnitude of the reduction was not as large as anticipated.

The model of the laminar zone at a cable-pipe contact lowered the

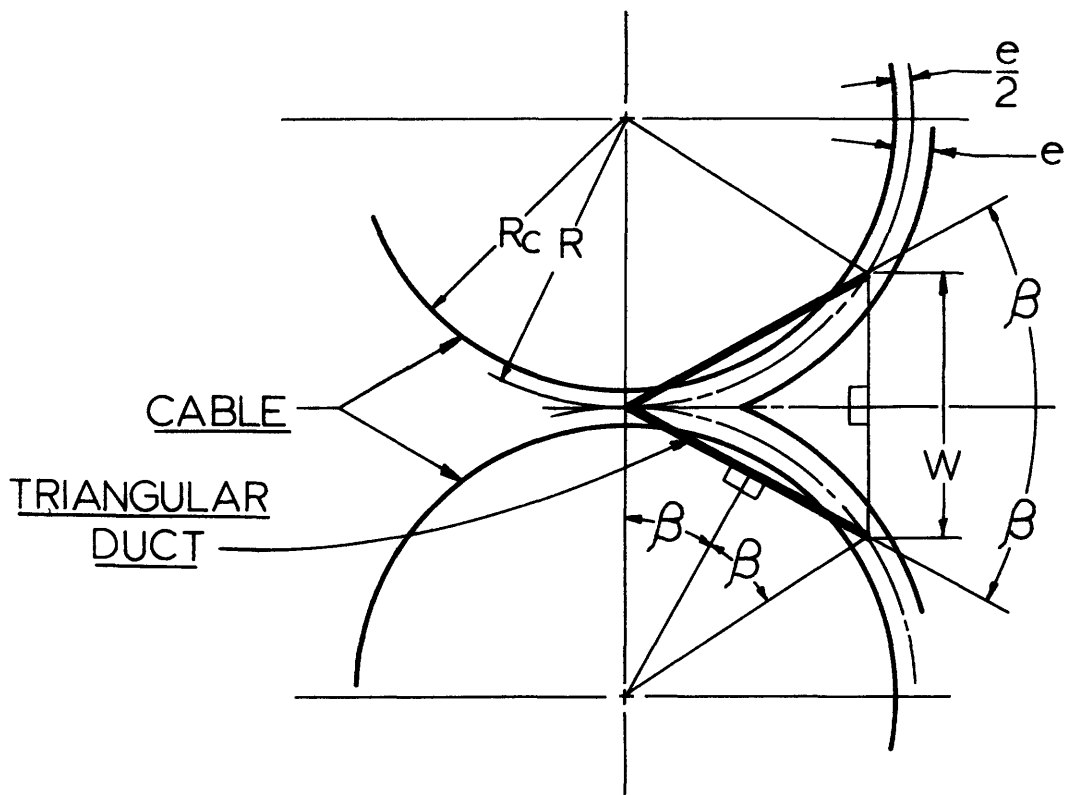


Figure 19. Cable-Cable Contact Point Showing Idealized Triangular Duct.

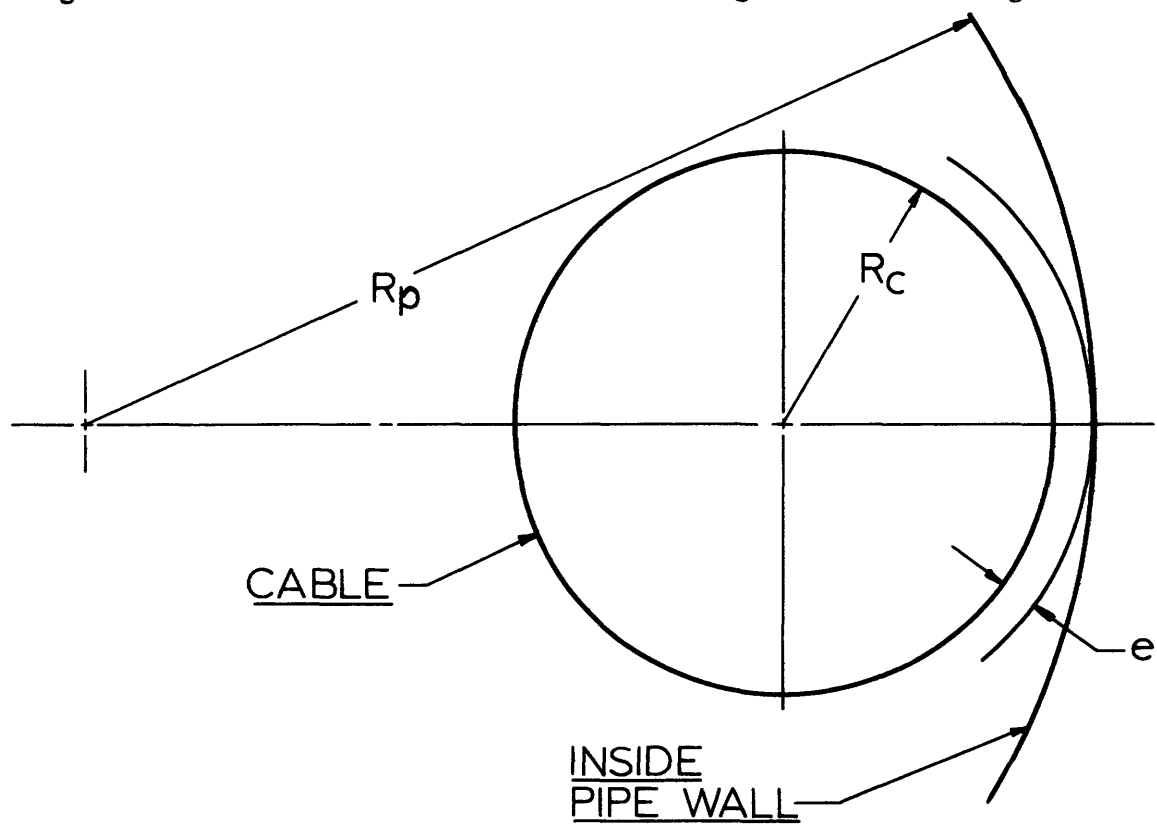


Figure 20. Cable-Pipe Contact

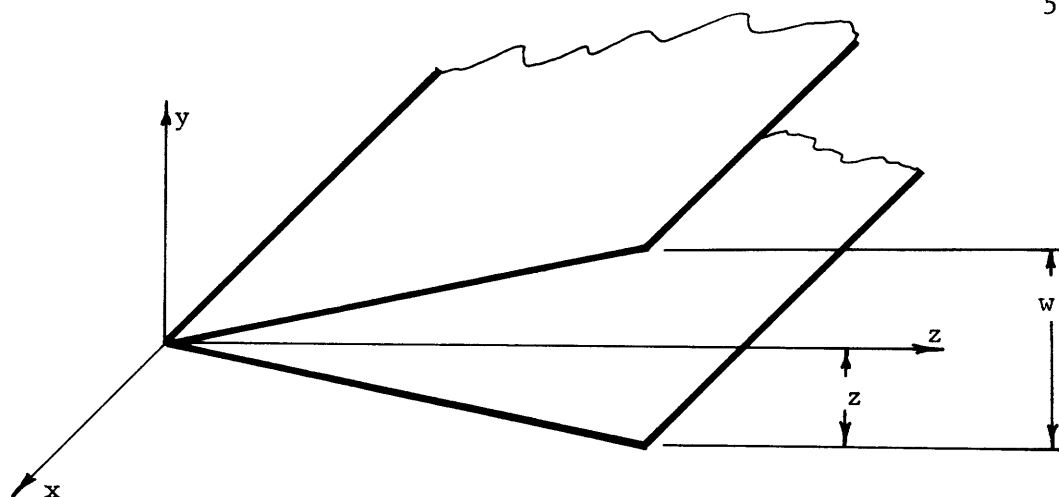


Figure 21. Co-Ordinate System of Triangular Duct

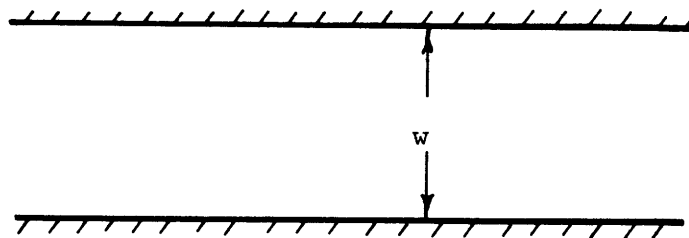


Figure 22. Two Infinite Parallel Plates Separated by Distance w .

friction factor too much, actually changing the slope of the friction factor vs. Reynolds number curve from negative to positive at low Reynolds numbers. The reason for this is attributed to the fact that the laminar zones were modelled as being triangular ducts and the cable-cable contact was close to this geometry while the cable-pipe contact was not. This is evident by referring to figures 19 & 20, and will become more evident as the development of the model progresses. This method will only be developed for a cable-cable contact since the cable-pipe contact was not accurate. The development of the method will be shown using configuration a.

The basic assumption of this theory is that the flow at a cable-cable contact may be approximated as being the same as the flow in a narrow, triangular, open ended duct, figure 21. For flow in such a duct, it has been shown by Eckert & Irvine [21] that laminar and turbulent flow may co-exist: the laminar flow being located near the apex of the duct, and at some point z away from the apex it changes to turbulent flow.

To find this point of transition, we first start out by defining a criteria for transition from laminar to turbulent flow. It is assumed that the flow which is very close to the transition point looks like the flow between two infinite parallel plates, as shown in figure 22. The hydraulic diameter for such a configuration is:

$$D_H = \frac{4A}{P} = \frac{4LW}{2L} = 2W \quad (34)$$

where w is the plate spacing. In laminar flow, the well accepted transition point from laminar to turbulent flow is 2000. Therefore, our criteria for transition is:

$$Re_{D_H} = \frac{\bar{V} D_H}{\nu} = \frac{\bar{V} (2w)}{\nu} = 2000 \quad (35)$$

$$\frac{\bar{V}_w}{\nu} = 1000 \quad (36)$$

We now need to know the average velocity \bar{V} between the parallel plates or across the duct at this position. From Eckert & Irving [21], the solution for the velocity for a triangular duct as shown in figure 21 for steady-state, laminar flow is:

$$v = \frac{-1}{2\mu} \left(\frac{dp}{dx} \right)_L \frac{z^2 \tan^2 \beta - y^2}{1 - \tan^2 \beta} \quad (37)$$

At any z , the average velocity across the cross section is:

$$\bar{V} = \frac{1}{z \tan \beta} \int_0^{z \tan \beta} \left(\frac{-1}{2\mu} \right) \left(\frac{dp}{dx} \right)_L \left(\frac{z^2 \tan^2 \beta - y^2}{1 - \tan^2 \beta} \right) dy \quad (38)$$

Performing the integration yields:

$$\bar{V} = \frac{-1}{12\mu} \left(\frac{dp}{dx} \right)_L \frac{w^2}{1 - \tan^2 \beta} \quad (39)$$

To find the pressure drop $(dp/dx)_L$, we make use of our basic assumption that the pressure drop is constant at any cross section. Therefore,

$$\left(\frac{dp}{dx} \right)_L = \left(\frac{dp}{dx} \right)_T = \frac{2 f_T \rho \bar{V}^2}{D_{HT}} \quad (40)$$

which may be rewritten as

$$\left(\frac{dp}{dx} \right)_L = \frac{2 f_T \rho \bar{V}_T^2}{D_{HT}} \frac{D_{HT}^2}{D_{HT}^2} \frac{v^2}{v^2} = \frac{2 f_T \rho v^2 (Re_{D_{HT}})^2}{D_{HT}^3} \quad (41)$$

Substituting (41) into (39) yields

$$\bar{V} = \frac{1}{6} \frac{f_T \nu Re_{DHT}^2 w^2}{D_{HT}^3 (1 - \tan^2 \beta)} \quad (42)$$

Substituting equ. (42) into our equation which gives us our criteria for transition, equ. (36), and solving for w yields:

$$w = \frac{18.171 D_{HT} (1 - \tan^2 \beta)^{1/3}}{f_T^{1/3} Re_{DHT}^{2/3}} \quad (43)$$

w may now be related to the angle β in figure 19 as follows:

$$w = 2 R (1 - \cos(2\beta)) \quad (44)$$

where $R = R_c + e/2$

Substituting equation (44) into (43) yields:

$$\frac{1 - \cos(2\beta)}{(1 - \tan^2 \beta)^{1/3}} = \frac{18.171 D_{HT}}{2 R f_T^{1/3} Re_{DHT}^{2/3}} \quad (45)$$

The procedure is to solve equation (45) for β using as the values of f_T , D_{HT} , and Re_{DHT} those which would be obtained if one assumed the flow to be completely turbulent without any laminar zones. Once the initial value of β is obtained, the area and perimeter of the laminar zones may be calculated. These values are then subtracted from the original turbulent values of area and wetted perimeter to obtain new values. This leads to a new value of hydraulic diameter for the turbulent flow

region. The friction factor and Reynolds number for the turbulent flow zone is then calculated using this new value of hydraulic diameter. The next step is to solve for the total friction factor, f_T , and Reynolds number, Re_T which is slightly more involved since the laminar regions must now be accounted for. These equations to obtain f_T and Re_T are now developed.

We begin by assuming that the pressure drop in the total pipe-type cable system is the same as in the turbulent region 12.

$$\left(\frac{dp}{dx}\right)_T = \left(\frac{dp}{dx}\right)_{12} \quad (46)$$

which may be written as,

$$\frac{f_T \bar{V}_T^2}{D_{HT}} = \frac{f_{12} \bar{V}_{12}^2}{D_{H12}} \quad (47)$$

It should be realized that the average total velocity, \bar{V}_T , is not equal to the average velocity in the turbulent zone, \bar{V}_{12} , since the average velocity in the turbulent zone is evidently not equal to the average velocity in the laminar zone, \bar{V}_L . Solving for f_T , we have:

$$f_T = f_{12} \left(\frac{\bar{V}_{12}}{\bar{V}_T}\right)^2 \left(\frac{D_{HT}}{D_{H12}}\right) \quad (48)$$

We must now find an expression relating \bar{V}_L to \bar{V}_T which is accomplished by use of the continuity equation:

$$\dot{m}_T = \dot{m}_{12} + \dot{m}_L \quad (49)$$

which may be written as:

$$A_T \bar{V}_T = A_{12} \bar{V}_{12} + 3 A_L \bar{V}_L \quad (50)$$

or, rearranging,

$$\frac{\bar{V}_T}{\bar{V}_{12}} = \frac{1}{A_T} \left[A_{12} + 3 \frac{\bar{V}_L}{\bar{V}_{12}} A_L \right] \quad (51)$$

which is the same as,

$$\frac{\bar{V}_T}{\bar{V}_{12}} = \frac{1}{A_T} \left[A_{12} + 3 \left(\frac{Re_L}{Re_{12}} \right) \left(\frac{D_{H12}}{D_{HL}} \right) A_L \right] \quad (52)$$

where D_{HL} is the hydraulic diameter of the laminar zone. The Reynolds number of the laminar zone, Re_L , is obtained as follows:

Assume:

$$\left(\frac{dp}{dx} \right)_{12} = \left(\frac{dp}{dx} \right)_L \quad (53)$$

which may be written as,

$$\frac{f_{12} \bar{V}_{12}^2}{D_{H12}} = \frac{f_L \bar{V}_L^2}{D_{HL}} \quad (54)$$

or

$$\frac{f_{12} Re_{12}^2}{D_{H12}^3} = \frac{f_L Re_L^2}{D_{HL}^3} \quad (55)$$

rewriting, we have,

$$Re_L^2 = \frac{f_{12}}{f_L} \frac{D_{HL}}{D_{H12}} Re_{12}^2 \quad (56)$$

We obtain f_L be beginning with the definition of the friction factor:

$$f_L = \left(\frac{dp}{dx} \right)_L \frac{D_{HL}}{2\rho \bar{V}_L^2} \quad (57)$$

dp/dx is obtained by beginning with the definition of the average velocity of the laminar zone, \bar{V}_L .

$$\bar{V}_L = \frac{Q_L}{A_L} \quad (58)$$

where Q_L is the volume rate of flow, and is obtained as follows:

$$Q_L = \int_{A_L} v \, dA_L \quad (59)$$

or

$$Q_L = \int_{z=0}^{z=z_0} \int_{y=0}^{y=z_0 \tan \beta} \left(\frac{1}{2\mu} \right) \left(\frac{dp}{dx} \right)_L \left(\frac{z^2 \tan^2 \beta - y^2}{1 - \tan^2 \beta} \right) dy \, dz \quad (60)$$

Integrating, we have,

$$Q_L = \frac{1}{6\mu} \left(\frac{dp}{dx} \right)_L \frac{z_0^4 \tan^3 \beta}{1 - \tan^2 \beta} \quad (61)$$

Substituting (61) into (58) we obtain,

$$\bar{V}_L = \frac{1}{6\mu} \left(\frac{dp}{dx} \right)_L \frac{z_0^2 \tan^2 \beta}{(1 - \tan^2 \beta)} \quad (62)$$

from figure 21 it is seen that $z_0 \tan \beta = w/2$, so we have,

$$\bar{V}_L = \frac{1}{6\mu} \left(\frac{dp}{dx} \right)_L \frac{(w/2)^2}{(1 - \tan^2 \beta)} \quad (63)$$

Equation (63) may be combined with equation (57) to eliminate $(dp/dx)_L$ and obtain.

$$f_L = \frac{12 (1 - \tan^2 \beta)}{Re_L} \quad (64)$$

Combining equation (64) and (56) to eliminate f_L , and solving for Re_L yields:

$$Re_L = \frac{f_{12} Re_{12}^2}{12 (1 - \tan^2 \beta)} \left(\frac{D_{HL}}{D_{H12}} \right)^3 \quad (65)$$

Now, combining equation (65) and (52) to eliminate Re_L , we have,

$$\frac{\bar{V}_T}{\bar{V}_{12}} = \frac{1}{Fr_T} \left[Fr_{12} + \frac{f_{12} Re_{12}}{4 (1 - \tan^2 \beta)} \left(\frac{D_{HL}}{D_{H12}} \right)^2 Fr_L \right] \quad (66)$$

Substituting equation (66) into equation (48), we now have an expression for f_T .

$$f_T = f_{12} \left[\frac{Fr_T^2 D_{HT}}{D_{H12} \left[Fr_{12} + \frac{f_{12} Re_{12}}{4 (1 - \tan^2 \beta)} \left(\frac{D_{HL}}{D_{H12}} \right)^2 Fr_L \right]^2} \right] \quad (67)$$

The overall Reynolds number Re_T is obtained by realizing that the following identity holds.

$$Re_T = Re_{12} \left(\frac{D_{HT}}{D_{H12}} \right) \left(\frac{\bar{V}_T}{\bar{V}_{12}} \right) \quad (68)$$

where \bar{V}_T/\bar{V}_{12} is obtained from equation (33). Combining (66) and (68), we have,

$$Re_T = Re_{12} \left(\frac{D_{HT}}{D_{H12}} \right) \frac{1}{f_T} \left[A_{12} + \frac{f_{12} Re_{12}}{4(1 - \tan^2 \beta)} \left(\frac{D_{HL}}{D_{H12}} \right)^2 A_L \right] \quad (69)$$

Equations (67) and (69) are the modified equations for f_T and Re_T which account for the laminar zones. It should be noticed that in the limit as the area of the laminar zone approaches zero ($Re_T \rightarrow \infty$), equations (67) and (69) reduce to identities. After (67) and (69) are solved for f_T and Re_T , then β is again solved for using equation (45). The areas and circumferences are then solved for again and from these, the new hydraulic diameters. Equations (67) and (69) are again solved and the process is continued until f_T and Re_T converge to their actual values.

Summarizing this procedure of calculating f_T and Re_T which includes the assumed laminar zones:

1. Calculate f_T and Re_T assuming the flow to be completely turbulent as outlined in Chapter III.
2. Determine β from equation (45).
3. Solve equations (67) and (69) for the new values of f_T and Re_T .
4. Return to step 2 until f_T and Re_T have converged.

The predictions of this method for configurations a & c are shown in figure 23. Also included in the figure are the predictions if the flow were assumed to be completely turbulent. It is seen that these laminar zones do indeed lower the predicted values; however, not in the manner that it was anticipated.

For configuration a, the left end of the curve was lowered too much whereas the right end was not lowered enough. For configuration c, the right end was lowered enough to agree perfectly with the experimental values for a short range and then are too low.

In view of the increased complexity to model the system with the assumption of the existence of laminar zones at points of contact, compared to the small improvement in the resulting predictions, it was decided not to use this as the final model.

EXPERIMENTAL DATA FOR MODEL FROM [1]

- - configuration b
- - configuration c

PREDICTED FROM THEORY FOR FULL SIZE MODEL

- configuration a - completely turbulent
- - - configuration a - with laminar zones
- configuration c - completely turbulent
- - - configuration c - with laminar zones

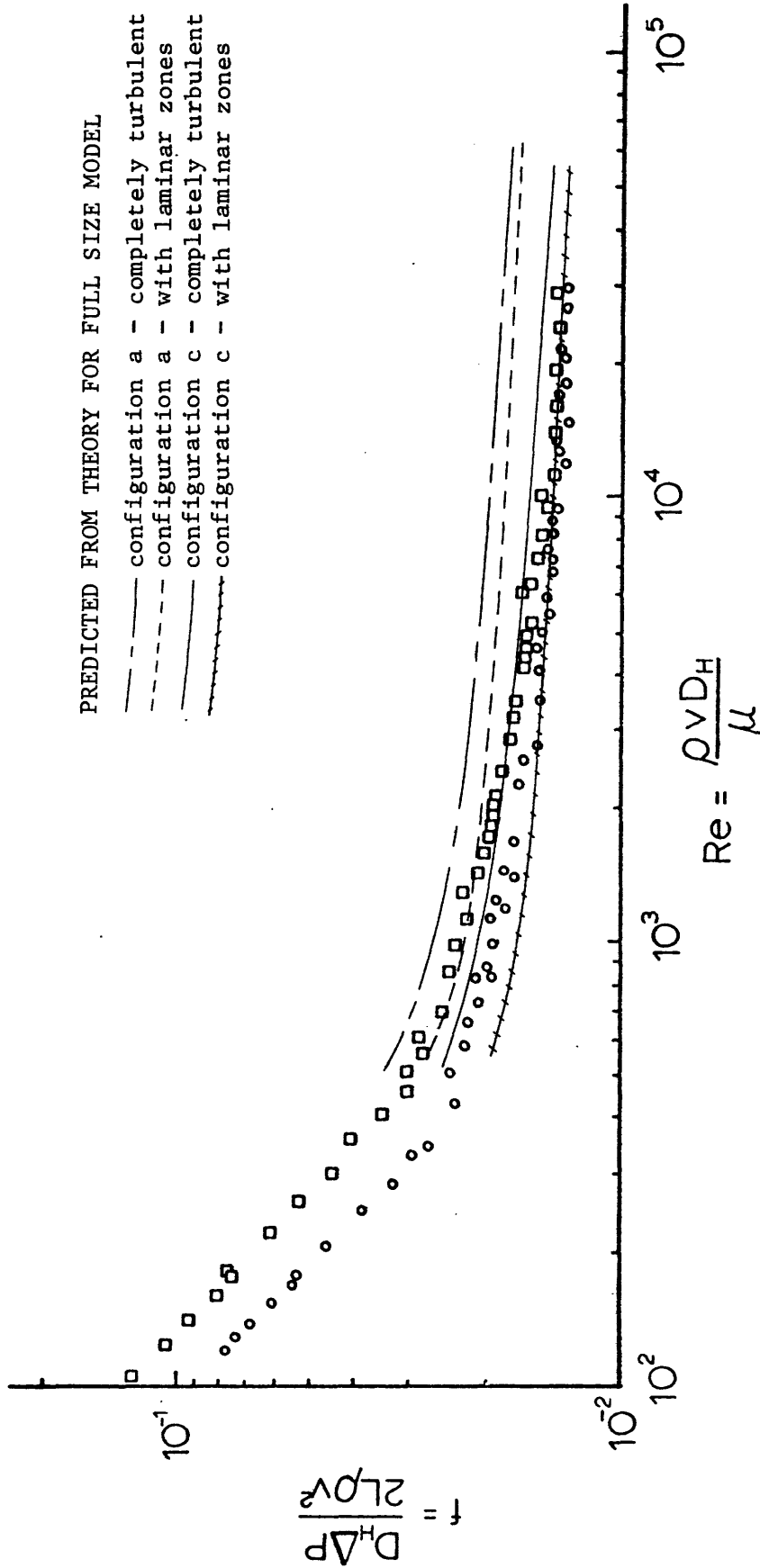


Figure 23. Theoretically Predicted Values when Points of Contact are Modelled as Laminar Zones.

CHAPTER VIII
PARAMETRIC STUDY

In our theory, the friction factor f has been found to be a function of the following parameters: p/e , D_c/D_p , e/D_c , and α . By inspecting the friction correlation for the rough surface (equ. (2)) the following should be evident:

1. Increasing p/e and α should decrease f_1 .
2. Decreasing D_c/D_p and e/D_c should decrease f_1 .

These effects will also be felt on the total friction factor f_T . The important aspects from a design standpoint is the degree to which these variations affect f_T . Probably the most practical question is what happens to f_T if one varies p , e , D_c , or α . The ultimate aim is to obtain a relation which predicts the variation of f_T relative to some reference position as a function of p , e , D_c , and α . The following system was chosen for study with D_p always being constant. This system corresponds to the standard 345 KV system.

$$D_p = 10.25''$$

$$D_c = 4.135''$$

$$p = 1.5''$$

$$e = 0.1''$$

$$\alpha = \tan^{-1} \left(\frac{np}{\pi D_c} \right); \text{ where } n = \# \text{ of skid wire starts} = 2$$

Varying D_c :

Varying D_c will vary D_c/D_p and e/D_c . Considering D_p to be a constant, the present practical range of interest would be to vary D_c/D_p from 0.35 to 0.40. The results are shown in figure 24. The effect of

EXPERIMENTAL DATA FOR MODEL FROM [1]

- - configuration b
- - configuration c

CONSTANTS

$D_p = 10.25''$

$p = 1.5''$
 $e = 0.1''$

D_c varies, therefore D_c/D_p and e/D_c vary

D_c/D_p	e/D_c	predicted from theory
0.40	0.024	—
0.38	0.025	---
0.35	0.028	---

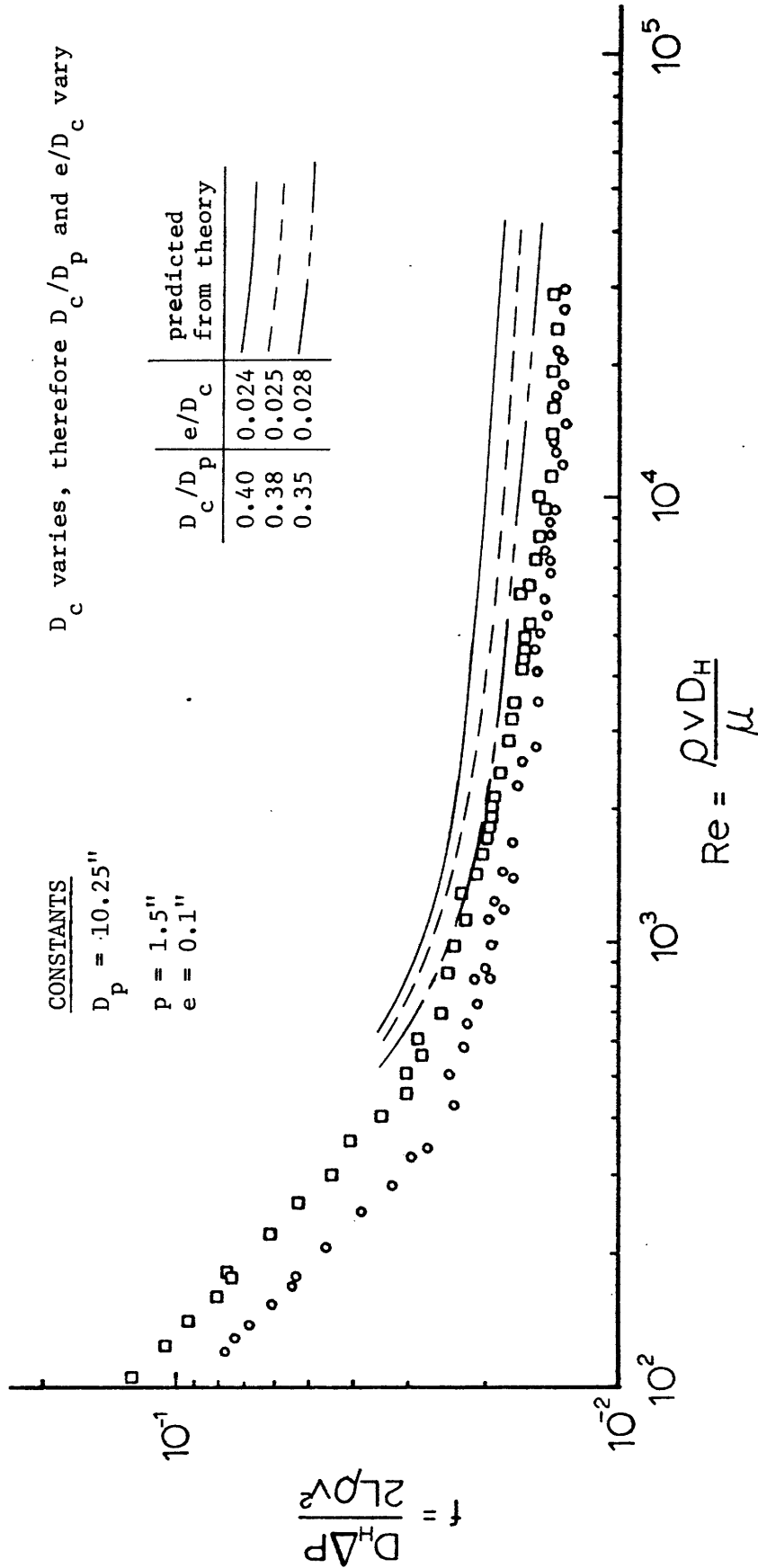


Figure 24 . Theoretically Predicted Results of Varying the Diameter of the Cable, D_c , in a Pipe-Type Cable Geometry.

decreasing D_c/D_p and D_c/e on f_T is as expected. A lower value of D_c/D_p means that there exists less rough surface to influence the flow, therefore, the friction factor should drop, as it indeed does. However, the extent of the reduction is not significant from a design viewpoint, especially since D_c is usually a constant specified by other criteria such as current capacity.

Varying the Helix Angle, α , by Increasing the Number of Skid Wire

Starts:

The helix angle, α , is defined as follows:

$$\alpha = \tan^{-1} \left(\frac{np}{\pi D_c} \right) ; \text{ where } n = \# \text{ of skid wire starts.}$$

For a fixed cable diameter, the helix angle may be varied by either changing the pitch or increasing the number of skid wire starts.

Increasing the number of skid wire starts will only vary the helix angle, α , not affecting any of the other important dimensionless parameters. By using the values of our chosen system, one could construct the following table relating the number of skid wire starts to the equivalent helix angle.

TABLE 1

NUMBER OF SKID WIRE STARTS AND CORRESPONDING HELIX ANGLE

<u># of starts</u>	<u>α (deg)</u>	<u>$K(\alpha)$ (from figure 9)</u>
1	6.6	0.91
2	13.0	0.89
4	24.8	0.82
8	42.7	0.62
16	61.0	0.37

The effect of increasing the helix angle, α , by increasing the number of skid wire starts is shown in figure 25. It is observed that the number of starts has to be greatly increased to yield a significant reduction in friction from the helix angle effect alone. Figure 25 was cross plotted to obtain the ratio of the friction factor f_T at any desired helix angle to the friction factor at a helix angle of zero degrees as a function of the helix angle α , for $\alpha > 15^\circ$.

$$\frac{f_T}{f_{T_0}} = (-.00875) \alpha + 1.135 \quad (70)$$

where α is in degrees. Evident from figure 25 is the fact that the effect on f_T of helix angle variations less than 15° is practically negligible.

Varying the pitch, p:

Varying p will vary p/e and α . The following table may be made for our system.

TABLE 2
VARYING THE PITCH, p

p (inches)	p/e	α (deg)	$K(\alpha)$ (from fig. 9)
1.0	10	8.8	0.9
1.5	15	13.0	0.89
3.0	30	24.8	0.82
4.0	40	31.6	0.75

It should be pointed out that the maximum helix angle is 31.6° . From figure 25, which shows the helix angle effect on f_T , it is evident that we should not expect a large variation in f_T to be caused by the helix

EXPERIMENTAL DATA FOR MODEL FROM [1]

- - configuration b
- - configuration c

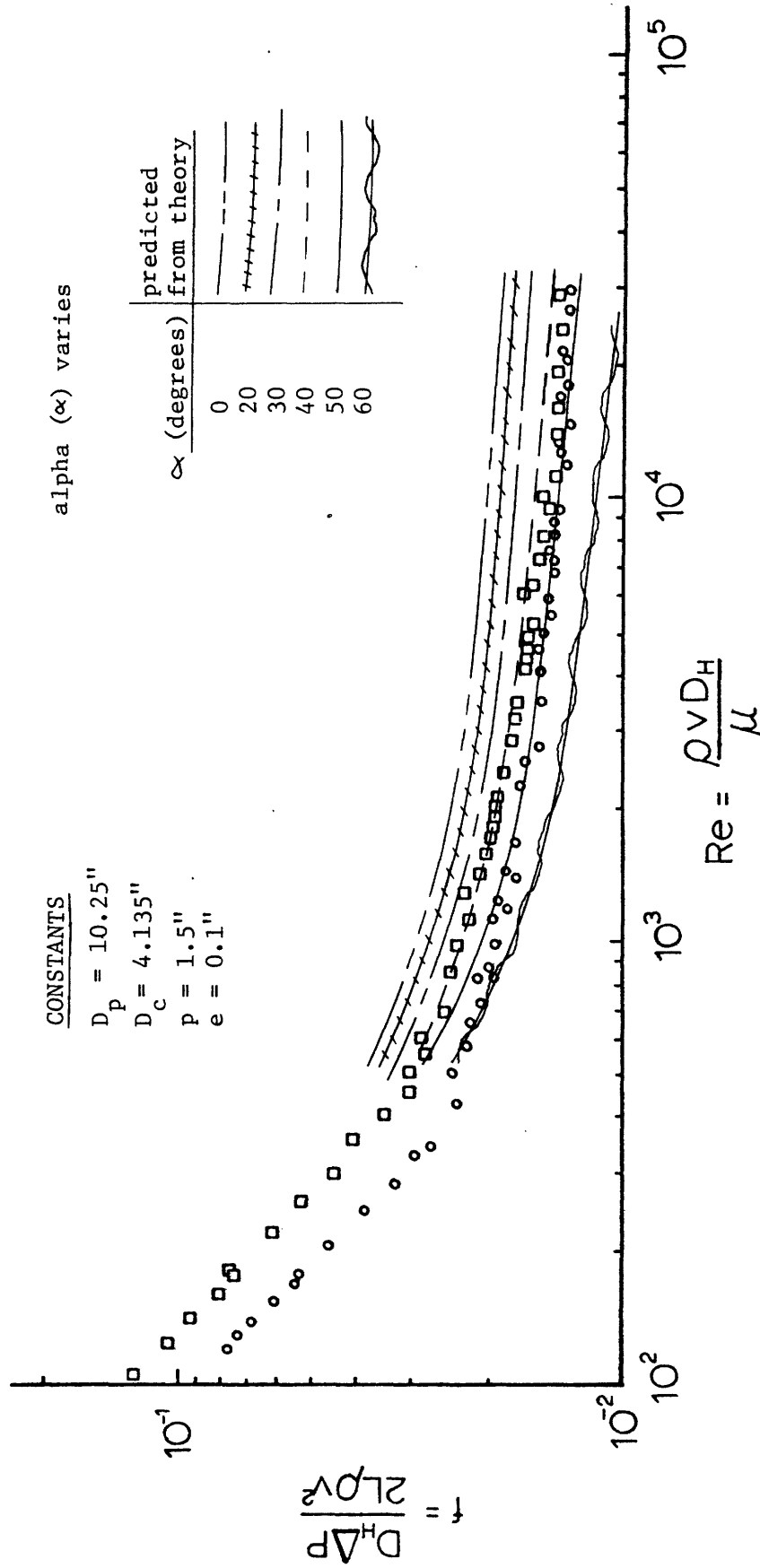


Figure 25 • Theoretically Predicted Results of Varying the Helix Angle, in a Pipe-Type Cable Geometry.

angle variation. Any significant variation in f_T should be attributed to the p/e variation.

The predictions for the variations in Table 2 are shown in figure 26. There is indeed quite an effect on f_T by varying the pitch, p , and as stated previously, this is attributed principally to the p/e variation, the helix angle variation being of secondary importance.

Varying e:

Varying e will vary p/e and e/D_c . The effect on f_T is severe and is shown in figure 27. For the present design, decreasing e by 50%, from 0.1 to 0.05 inches, will yield a 39% reduction in friction factor which is essentially independent of Reynolds Number.

In order to obtain a correlation relating the variation of f_T/f_{T0} as a function of p/e and e/D_c , it is necessary to isolate the effect each has on f_T/f_{T0} . This is accomplished by varying e and p simultaneously to keep the ratio p/e constant and observing the effect of the variation of e/D_c on f_T . The results are shown plotted in figure 28. By cross plotting these results, the following equation may be obtained:

$$\frac{f_T}{f_{T0}} = 4.337 \left(\frac{e}{D_c} \right)^{0.387} \quad (71)$$

where f_{T0} corresponds to the value of friction factor for our standard 345 KV system. This equation may now be used to account for the contribution of the e/D_c variation in figure 27 and determine the effect of the p/e contribution. The resulting correlation for the variation of f_T/f_{T0} due to a variation in e at constant α is:

EXPERIMENTAL DATA FOR MODEL FROM [1]

- - configuration b
- - configuration c

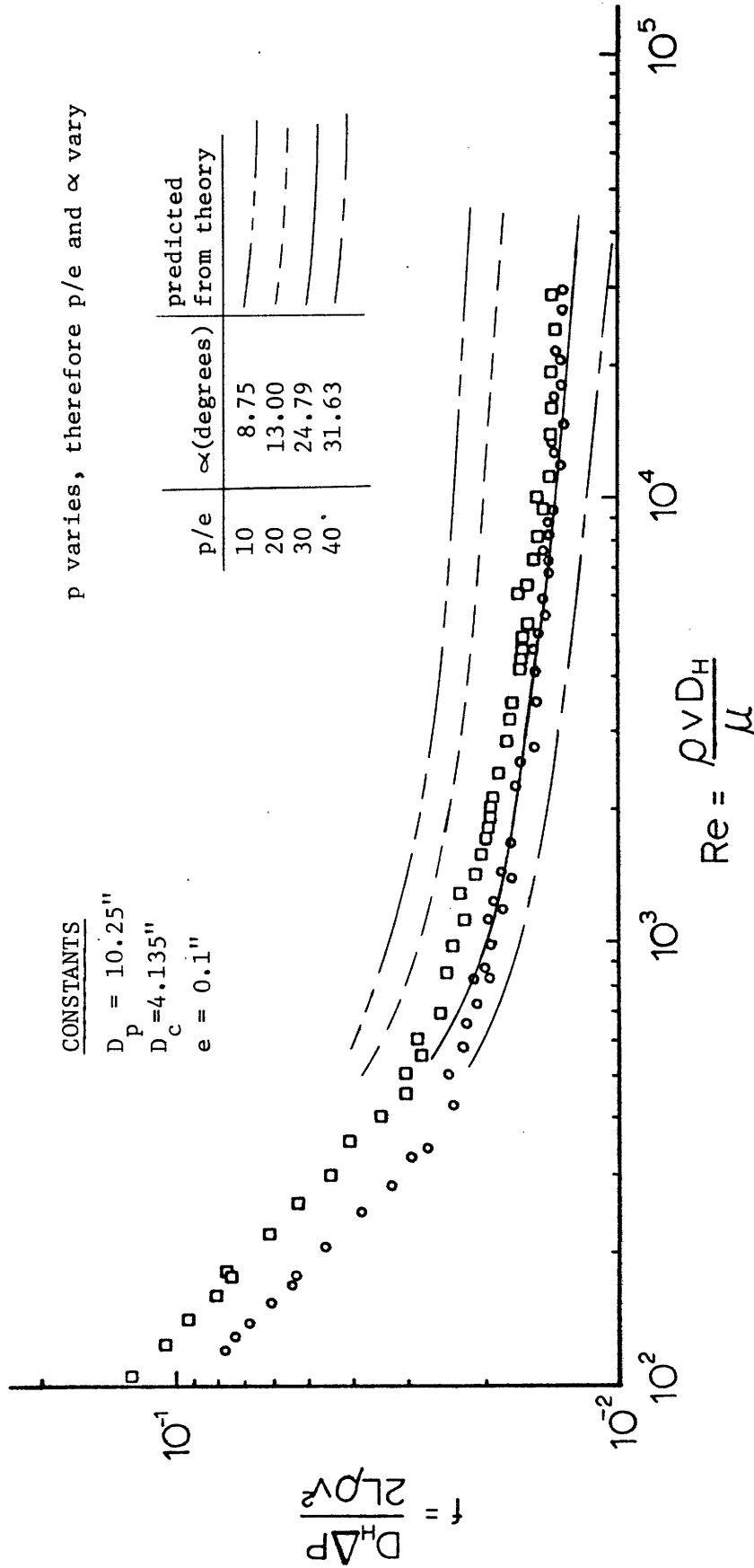


Figure 26. Theoretically Predicted Results of Varying the Pitch, p , in a Pipe-Type Cable Geometry.

EXPERIMENTAL DATA FOR MODEL FROM [1]

- - configuration b
- - configuration c

CONSTANTS

$D_p = 10.25''$

$D_c = 4.135''$

$p = 1.5''$

e varies, therefore p/e and e/Dc vary

p/e	e/D _c	predicted from theory
10	0.036	
11.53	0.031	
15	0.024	
18.75	0.019	
30	0.012	
37.5	0.010	

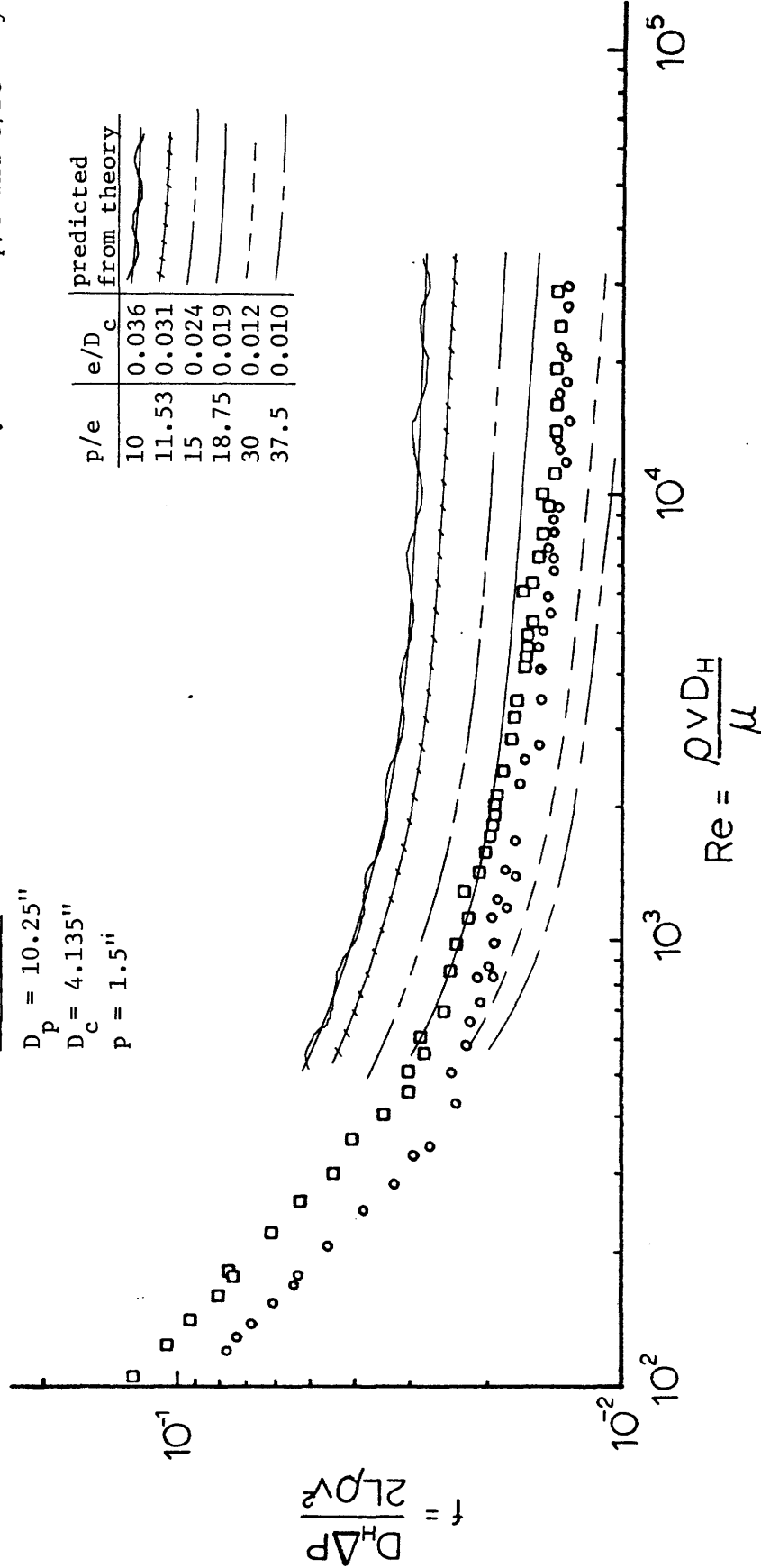


Figure 27. Theoretically Predicted Results of Varying the Height of the Skid Wire, e, in a Pipe-Type Cable Geometry.

EXPERIMENTAL DATA FOR MODEL FROM [1]

- - configuration b
- - configuration c

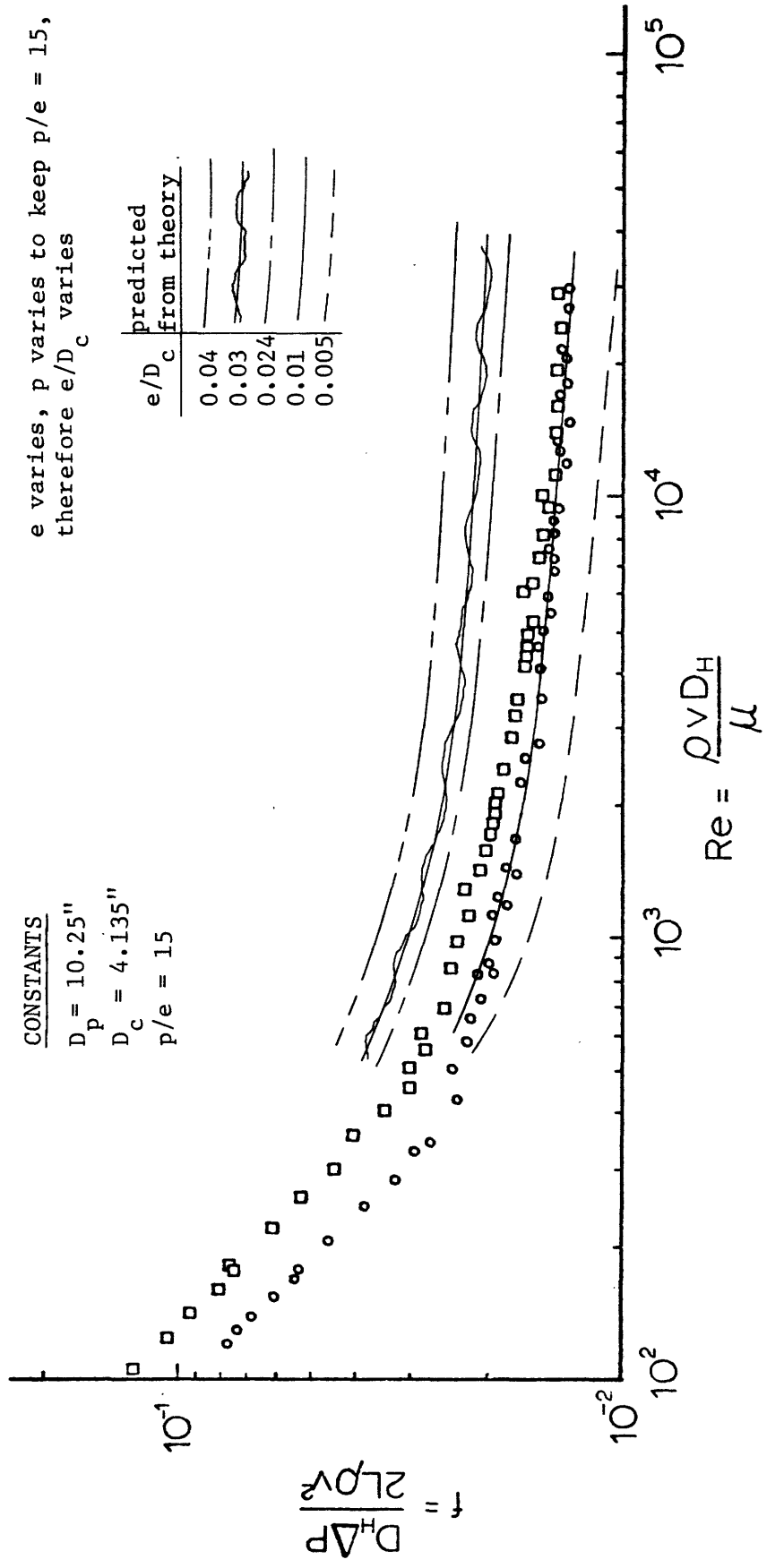


Figure 28. Theoretically Predicted Results of Varying e While Keeping p/e constant in a Pipe-Type Cable Geometry.

$$\frac{f_T}{f_{T_0}} = 12.273 \left(\frac{e}{D_c}\right)^{.387} \left(\frac{P}{e}\right)^{-.373} \quad (72)$$

Final Correlation:

The most important design parameters have been found to be p/e , e , and α . These have been found to be of importance in the following forms: p/e , e/D_c , α . Equation (72) contains p/e and e/D_c as independent variables and is independent of α . Equation (70) accounts for the variation in α and is independent of p/e and e/D_c . These two equations may be combined to yield an equation which will predict the variation f_T/f_{T_0} as a function of p/e , e/D_c , and α which is:

$$\frac{f_T}{f_{T_0}} = 12.273 \left(\frac{e}{D_c}\right)^{.387} \left(\frac{P}{e}\right)^{-.373} \quad \text{for } \alpha < 15^\circ \quad (73a)$$

$$\frac{f_T}{f_{T_0}} = 12.273 \left(\frac{e}{D_c}\right)^{.387} \left(\frac{P}{e}\right)^{-.373} \left[(-.00875) \alpha + 1.135 \right] \quad \text{for } \alpha > 15^\circ \quad (73b)$$

where α is in degrees.

It should be noticed that equation (73) does not include any variation for helix angle variations below 15° since they were found to be negligible. To include the correction for variations in D_c/D_p the value used for f_{T_0} should be the appropriate one taken from figure 24.

With regard to the accuracy of the above equation, it should be remembered that this parametric study was performed using configuration b which predicts values which are approximately 15% too high in the range of interest ($Re \approx 500$). The author believes that equation (73) is accurate to within $\pm 5\%$ of the actual predicted value. Therefore, the

predictions range from 10% - 20% too high in the Reynolds Number range of interest to 25% - 35% too high at high Reynolds Numbers ($Re > 3000$).

Also deserving some discussion is the fact that the theory predicts a uniform variation essentially independent of Reynolds number as one or more parameters are varied. This is reasonable at high Reynolds numbers, but at low Reynolds numbers, there is a question as to whether this is actually the case. It would seem more reasonable that as one approached the transition region ($Re \approx 500$) that all of the predictions from the theory should merge since in the laminar region the skid wire geometry is unimportant in determining the friction factor. This assumption may be checked by further experimental tests varying the parameters as shown in figure 27.

CHAPTER IX

RESULTS AND CONCLUSIONS

A method has been developed which will predict the friction factor for turbulent flow in a pipe-type cable system. Four different configurations were modelled and the predicted values are dependent upon which one of the four is used. Using the most conservative model, the predictions are consistently 15% - 30% too high.

In the laminar flow regime, viscous forces predominate and any disturbances introduced in the flow are completely damped out, which means that the skid wires do not have any influence in this regime. As the Reynolds Number is continually increased, the inertia forces begin to increase as the viscous forces decrease. When the viscous forces are no longer strong enough to damp out any instabilities which occur due to the presence of the skid wires, the laminar flow becomes turbulent and the skid wires must now be considered in the analysis of determining the flow characteristics.

In the turbulent flow regime, the friction factor f_T has been found to be a function of the following parameters: p/e , D_c/D_p , e/D_c , and α . If one assumes that for a given system, specifications fix the values of D_c and D_p , then we have three parameters to vary in order to try and reduce f_T . These are the skid wire pitch, p , the height of the skid wire, e , and the helix angle of the skid wire on the cable, α , where $\alpha = \tan^{-1} \frac{np}{\gamma D_c}$: where $n = \#$ of skid wire starts. From the parametric study performed in the last chapter, the following are evident:

1. Varying e will produce the greatest effect of any other param-

eter on f_T , as shown in figure 27. For the present case, decreasing e by one half, from 0.1 inches to 0.05 inches will yield a 39% reduction in friction factor which is essentially independent of Reynolds number.

2. Increasing the skid wire pitch, p , will reduce f_T . For the present case, a doubling of the pitch from 1.5 to 3.0 inches will reduce f_T by 30% which is essentially independent of Reynolds Number.
3. The number of skid wire starts must be increased considerably to substantially reduce f_T . Increasing the number of skid wire starts from 2 in the present case to 16 would yield a 40% reduction in f_T which is essentially independent of Reynolds number. This would not be a realistic way of reducing f_T .

f_T is related to the parameters p , e , and α by the relationship

$$\frac{f_T}{f_{T_0}} = 12.273 \left(\frac{e}{D_c}\right)^{.387} \left(\frac{p}{e}\right)^{-.373} \quad \text{for } \alpha < 15^\circ \quad (73a)$$

$$\frac{f_T}{f_{T_0}} = 12.273 \left(\frac{e}{D_c}\right)^{.387} \left(\frac{p}{e}\right)^{-.373} \left[(-0.00875) \alpha + 1.135 \right] \quad \text{for } \alpha > 15^\circ \quad (73b)$$

The previous equations are believed to predict values of f_T which are from 10% - 20% above the actual values for Reynolds numbers below 3000 and from 25% - 35% above the actual values for Reynolds numbers above 3000.

CHAPTER XI
RECOMMENDATIONS

It is recommended to perform further experiments with the parameter variations similar to the variations in figure 27 to find what actually happens at low Reynolds Numbers to the friction factor curve. The user may also want to modify the program to output the average of the predictions for configurations b & c as suggested at the end of Chapter VI

REFERENCES

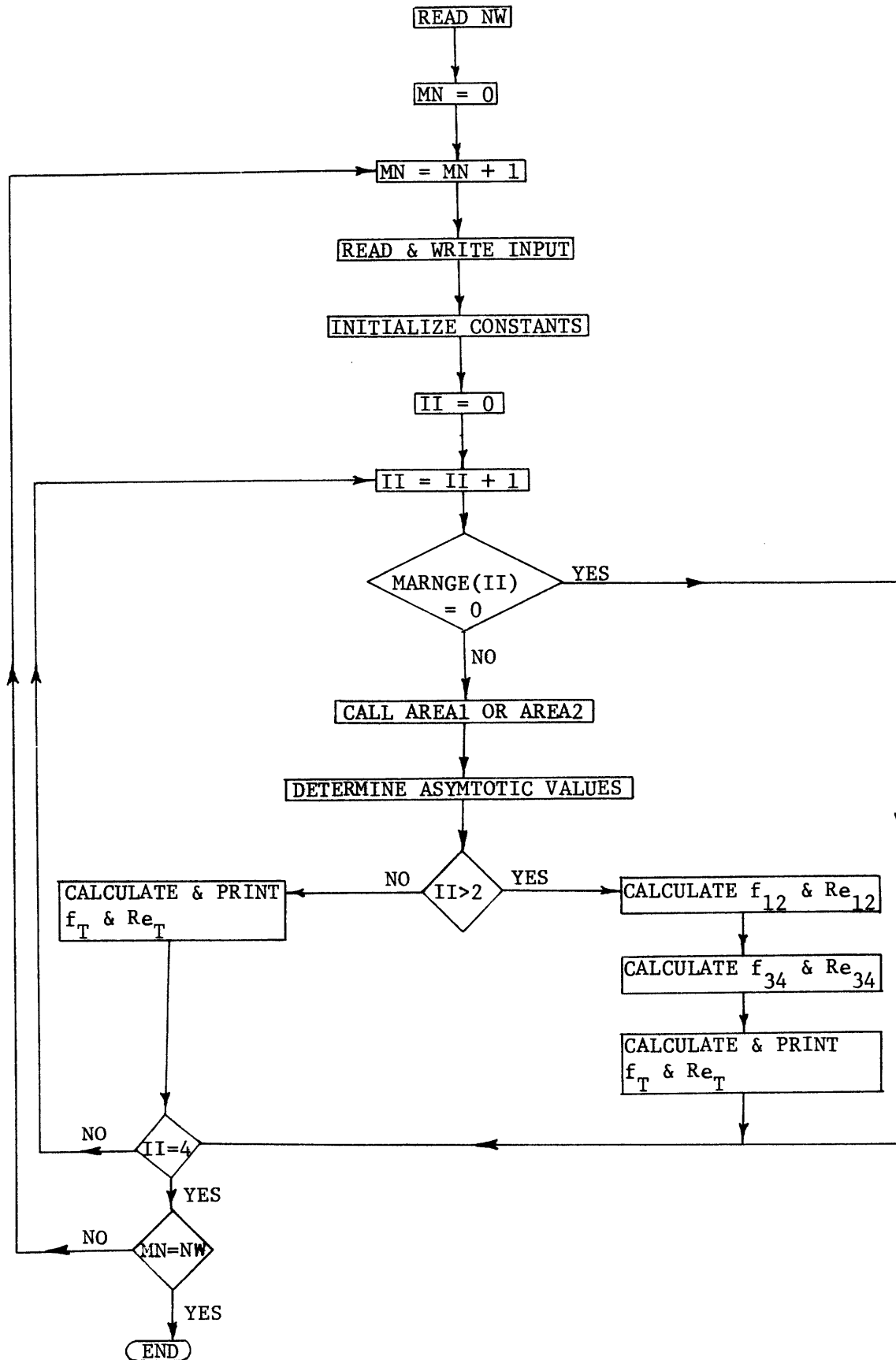
1. Slutz, R.A., Glicksman, L.R. and Rohsenow, W.M., "Cooling of Underground Transmission Lines", Heat Transfer Laboratory, M.I.T. DSR-80610-83, July, 1973.
2. Hall, W.B., Heat Transfer in Channels Having Rough and Smooth Surfaces," Journal of Mechanical Engineering Science, Vol. 4, No. 3, 1962, pp. 287-291. also, IGR-TN/W.832 (1958).
3. Wilkie, D., "Forced Convection Heat Transfer from Surfaces Roughened by Transverse Ribs, Paper No. 1. Third International Heat Transfer Conference Proc., Aug. 7-12, 1966.
4. Wilkie, D., "Calculation of Heat Transfer and Flow Resistance of Rough and Smooth Surfaces Contained in a Single Passage", Paper No. 2, Third International Heat Transfer Conference Proc., Vol.1, Aug. 7-12, 1966.
5. Wilkie, D., Cowin, M., Burnett, P., and Burgoyne, T., "Friction Factor Measurements in a Rectangular Channel With Walls of Identical and Non-Identical Roughness," International Journal of Heat and Mass Transfer", Vol. 10, 1967, pp. 611-621.
6. Wilkie, D., and White, L., "Calculation of Flow Resistance of Passages Bounded by a Combination of Rough and Smooth Surfaces", Journal Br. Nucl Energy Soc, 6, No. 1, 1967.
7. Walker, V. and Wilkie, D., "The Wider Application of Roughened Heat Transfer Surfaces as Developed for Advanced Gas-Cooled Reactors", Symposium on High Pressure Gas as a Heat Transfer Medium, London, March 9-10, 1967, Paper No. 26, Inst. of Mech Eng. Proc.
8. Kjellstrom, B. and Hedberg, S., "On Shear Stress Distributions for Flow in Smooth or Partially Rough Annuli, EAES Heat Transfer Symposium, Bern (August 1966), Report AE-243 (1966).
9. Sheriff, N. and Gumley, P., "Heat Transfer and Friction Properties of Surfaces with Discrete Roughness", International Journal of Heat and Mass Transfer," Volume 9, 1966, pp. 1297-1320.
10. White, W.J. and White, L., "The Effect of Rib Profile on Heat Transfer and Pressure Loss Properties of Transversely Ribbed Roughened Surfaces", ASME Conference Proc., N.Y., 1970.
11. White, L. and Wilkie, D. "The Heat Transfer and Pressure Loss Characteristics of Some Multi-Start Ribbed Surfaces", ASME Conf., N.Y. 1970.

12. Maubach, K., "Rough Annulus Pressure Drop-Interpretation of Experiments and Recalculation for Square Ribs", International Journal of Heat and Mass Transfer, Vol. 15, 1972, pp. 2489-2498.
13. Cope, W.F., "The Friction and Heat-Transmission Coefficients of Rough Pipes", Proc, Instn. Mech. Engrs., Vol. 145, 1941, pp. 99-105.
14. Sams, E.W., "Experimental Investigation of Average Heat Transfer and Friction Coefficients for Air Flowing in Circular Pipes Having Square Thread Type Roughness," NACA RM-E 52D17, 1952.
15. Sams, E.W., "Heat Transfer and Pressure Drop Characteristics of Wire-Coil-Type Turbulence Promoters", Reactor Heat Transfer Conference of 1956, USAEC Technical Information Service Extension, Oak Ridge, Tenn TID-7529 (Pt. 1) Book 2, Physics and Mathematics, 1957, pp. 390-415.
16. White, F.M., "Viscous Fluid Flow". McGraw-Hill, New York, 1974.
17. Webb, R.L., Eckert, E.R.G., and Goldstein, R.J., "Heat Transfer and Friction in Tubes with Repeated-Rib Roughness," International Journal of Heat and Mass Transfer, Vol. 14. No. 4, April 1971, pp. 601-616.
18. Moody, L.F., "Friction Factors for Pipe Flow", Transactions of the ASME, Vol. 66, November 1944, pp. 671-684.
19. Schlichting, H., "Boundary Layer Theory", 6th Ed. McGraw-Hill, New York, 1968.
20. Feurstein, G., und Rampf, H., "Der Einfluss rechteckiger Rouhigkeiten auf den Wärmeübergang und den Druckabfall in turbulenter Ringspaltromung" Wärme-und Stoffübertragung 2(1), 19-26 (1969).
21. Eckert, E.R.G. and Irvine, T.F., Jr., "Flow in Corners of Passages with Noncircular Cross Sections," Trans. ASME, Vol. 78, May 1956, pp. 709-718.
22. Plapp, J.E., "Engineering Fluid Mechanics", Prentice-Hall, Englewood Cliffs, N.J., 1968.
23. Sabersky, R.H., Acosta, A.J., and Hauptmann, E.G., "Fluid Flow", 2nd ed. 1971, Macmillan Co. N.Y. 1964.
24. Rohsenow, W.M., and Choi, H., "Heat Mass and Momentum Transfer", Prentice-Hall, Englewood Cliffs, N.J., 1961.
25. Edwards, F.J. and Sheriff, N., "The Heat-Transfer and Friction Characteristics for Forced-Convection Heat Flow Over a Particular Type of Rough Surface", 1961-1962 Heat Transfer Conference Proc., University of Colorado, Boulder, 1961.

27. Bandopadhyay, P.C. and Hinwood, J.B., "On the Coexistence of Laminar and Turbulent Flow in a Narrow Triangular Duct," Journal of Fluid Mechanics, Vol. 59, Part 4, 1973, pp. 775-783.
28. Kokorev, L.S., Korsun, A.S., Kostyunin, B.N. and Petrovichev, V.I., "Hydraulic Drag and Heat Transfer in Turbulent Flow of Liquids in Triangular Channels", Heat Transfer-Soviet Research, Vol. 3, No.1, January-February, 1971, pp. 56-65.
29. Carlson, L.W. and Irvine, T.F., Jr., "Fully Developed Pressure Drop in Triangular Shaped Ducts", Journal of Heat Transfer, Vol. 83, November 1961, pp. 441-444.

APPENDIX A

FLOW CHART OF COMPUTER PROGRAM



APPENDIX B

DEFINITION OF VARIABLES USED IN THE COMPUTER PROGRAM

ARRAYS:

MARNGE () - designates which configuration the program is going to model

MARNGE (1) = configuration a

MARNGE (2) = configuration b

MARNGE (3) = configuration c

MARNGE (4) = configuration d

The values in the array (either a zero or a one) are read as input into the program. If MARNGE (I) = 0 (where I = 1,2,3, or 4), then the program will not model the configuration corresponding to MARNGE(I). If MARNGE(I) = 1, then the program will model the appropriate configuration.

X12(,) - storage array for region 12 when either configuration c or d is to be modelled.

$$X12(1,I) = f_{12}^{0.5} Re_{12}/D_{12}^{1.5} \text{ (left hand side of equ. (33))}$$

$$X1w(2,I) = Re_{12}$$

$$X12(3,I) = f_{12}$$

X34(,) - storage array for region 34 when either configuration c or d is to be modelled.

$$X34(1,I) = f_{34}^{0.5} Re_{34}/D_{34}^{1.5} \text{ (right hand side of equ. (33))}$$

$$X34(2,I) = Re_{34}$$

$$X34(3,I) = f_{34}$$

SUBROUTINES:

AREA1 - computes the circumferences, areas, and hydraulic diameters
for configurations a & b.

AREA2 - computes the circumferences, areas, and hydraulic diameters
for configurations c & d.

INPUT PARAMETERS:

The following parameters are read in as input to the program from data cards.

- MARNGE() - array which is described in section ARRAYS
- NW - specifies the number of different geometrically different configurations to be modelled.
- DP - diameter of the pipe
- DC - diameter of the cable taken from the base of the skid wires
- P - pitch of skid wire lay
- E - height of skid wire
- ADJUST - the value of $K(\alpha)$ taken from figure 7. ($\alpha = \tan^{-1}(\frac{nP}{wDc})$;
where n = number of skid wire starts).

COMPUTATION PARAMETERS:

The following are the most important parameters which are used in the program for computation purposes.

- PI - 3.141593
- RP - radius of the pipe
- RC - radius of the cable
- DASYM1 - asymptotic value of hydraulic diameter as Reynolds number approaches infinity for region 12 for all configurations.
- DASYM3 - asymptotic value of hydraulic diameter as Reynolds number approaches infinity for region 34 for configurations c & d.
- hydraulic diameter of region 3 for configuration b.
(constant for all Reynolds numbers).
- RE12 - Reynolds number for region 12
- RE34 - Reynolds number for region 34
- F12 - friction factor for region 12
- F34 - friction factor for region 34
- F3 - friction factor for region 3
- D12 - hydraulic diameter of region 12 (constant)
- D34 - hydraulic diameter of region 34 (constant)
- D1 - initially the asymptotic value of hydraulic diameter for region 12 as Reynolds number approaches infinity - DASYM1 (from equ (12) with $D_{H2} = 0$). Decreases by amount DINCR after each f_{12} and corresponding Re_{12} are computed. D1 is the independent variable described in the computation procedure of Chapter III.
- D3 - the same as D1 except for region 34.

DINCR - the increment that is to be subtracted from D1 or D3
after either f_{12} and Re_{12} or f_{34} and Re_{34} are calculated.

OUTPUT PARAMETERS:

The following are the computed output parameters.

- RET - Reynolds number for the entire pipe-type geometry.
- FT - Corresponding friction factor for the entire pipe-type geometry.

APPENDIX CUSERS INSTRUCTIONS FOR COMPUTER PROGRAM

For any pipe-type cable system, only five parameters must be specified as input to the program, which are listed below.

1. Dp - diameter of the pipe
2. Dc - diameter of the cable
3. P - skid wire pitch
4. e - skid wire height
5. K(α) - correction coefficient to equation (2) obtained from figure 9.

α is defined from the following equation: $\alpha = \tan^{-1} \left(\frac{n P}{\pi D_c} \right)$

where n = number of skid wire starts.

The units of Dp, Dc, P, and e are arbitrary; however, they must be consistent. Each pipe-type geometry, specified by a unique combination of the five input parameters described above, require three data cards. In addition, the first data card for every computer run specifies the number of different pipe-type arrangements to be modelled (i.e., the number of groups of data cards; each group containing three cards as described above). The variable read in from this first data card is read in under INTEGER FORMAT and must be right justified. Table 3 describes these input data cards in more detail:

TABLE 3
DATA CARD ASSEMBLY

<u>Card</u>	<u>Column(s)</u>	<u>Variable</u>	<u>Format</u>
1	1 - 2	NW	I
2	1 - 7	D _p	F
2	8 - 14	D _c	F
2	15 - 21	p	F
2	22 - 28	e	F
3	1	MARNGE(1)	I
3	2	MARNGE(2)	I
3	3	MARNGE(3)	I
3	4	MARNGE(4)	I
4	1 - 7	K	F

NW TOTAL GROUPS →

Total Number of Data Cards = $1 + 3(NW)$; therefore, there must exist at least four (4) data cards.

APPENDIX D

SOURCE LISTING

```

0001 DIMENSION MARNGE(4)
0002 DIMENSION X12(3,101),X34(3,101)
0003 IR = 5
0004 IW = 6
0005 REAC(IR,802)NW
0006 DO 999 MN = 1,NW
0007 REAC(IR,800)DP,DC,P,E
0008 REAC(IR,801)MARNGE
0009 REAC(IR,800)ADJUST
0010 FORMAT(4F7.4)
0011 800
0012 801 FORMAT(7I1)
0013 802 FORMAT(I2)
0014 WRITE(IM,18)
0015 WRITE(IM,504)
0016 FORMAT(//,5X,3('*****'),INPUT,3('*****'),//)
0017 WRITE(IM,505)DC
0018 FORMAT(/,5X,'DIAMETER OF CABLE = ',F7.4,' INCHES')
0019 WRITE(IM,506)CP
0020 FORMAT(5X,'DIAMETER OF PIPE = ',F7.4,' INCHES')
0021 WRITE(IM,507)P,E
0022 FORMAT(5X,'P = ',F6.3,' INCHES',/,5X,'E = ',F7.5,' INCHES')
0023 PE = P/E
0024 WRITE(IM,508)PE
0025 FORMAT(5X,'PITCH TO HEIGHT RATIO (P/E) = ',F8.4)
0026 DO 15 J = 1,4
0027 15 WRITE(IM,510)J,MAFACE(J)
0028 510 FORMAT(5X,'MARNGE(',I1,') = ',I1)
0029 WRITE(IM,512)ADJUST
0030 512 FORMAT(5X,'ADJUST = ',F9.4)
0031
0032 C
0033 C
0034 C
0035 INITIALIZE CONSTANTS
0036 PI = 3.141593
R = -3.75 + C.95*(P/E)**0.53
S = 2.0/0.C791
SI = 2.0/0.046

```

```

0037
0038
0039
0040
0041
0042
0043
0044
0045
0046
0047
0048
0049
0050
0051
0052
0053
0054
0055
0056
0057
0058
0059
0060
0061
0062
0063
0064
0065
0066
0067
0068
0069
0070
0071
0072

RP = DP/2.
RC = DC/2.
SUBC = (E/P)**C.53

CC 105 II = 1,4
IF(MARNGE(II).EQ.0) GC TO 105
IF(II.LT.3) CALL AREA1(IM,II,RC,RP,A12,A3,AT,C1,C2,C3,D12M,D3,DHT)
IF(II.GE.3) CALL AREA2(IM,II,RC,RP,A12,A34,AT,C1,C2,C3,C4,D12M,
*D34M,DHT)
D12 = D12M

C *****
C ASYMTOTIC VALUES *****
C
DASYM1 = 4.0*A12/C1
F1 = 2.5*ALOG(DASYM1/(2.*E)) - 3.75
F1 = F1 + .95*(P/E)**0.53
F1 = 2./(F1*F1)
F1 = F1*ADJUST
F12 = (C12/DASYM1)*F1
IF(II.NE.2) GO TO 9
DASYM3 = 4.0*A3/C3
F3 = 2.5*ALOG(DASYM3/(2.*E)) - 3.75
F3 = F3 + .95*(P/E)**.53
F3 = 2./(F3*F3)
F3 = F3*ADJUST
R3OR12 = ((F12/F3)**0.5)*((D3/D12)**1.5)
FT = A12 + 2.*F3CR12*C12*A2/C2
FT = AT*AT/(FT*FT)
FT = FT*F12*DHT/D12
9 CONTINUE
IF(II.LT.3) GC TO 25
DASYM3 = 4.0*A34/C3
F3 = 2.5*ALOG(DASYM3/(2.*E)) - 3.75
F3 = F3 + .95*(P/E)**.53
F3 = 2./(F3*F3)

```

```

0073
0074
0075
0076
0077
0078
0079
0080
0081
0082
0083
0084
0085
0086
0087
0088
0089
0090
0091
0092
0093
0094
0095
0096
0097
0098
0099
0100
0101
0102
0103
0104
0105
0106
0107
0108

F34 = (D34M/DASYM3)*F3
R34D12 = ((F12/F34)*C.5)*((D34M/D12M)*1.5)
FT = A12 + 2.*R34C12*D124*A24/D34M
FT = AT*AT/(FT*FT)
FT = FT*F12*DH1/D124
25 CONTINUE
WRITE(IH,16)II
16 FORMAT(////,10X,'ASYMPTOTIC VALUES AS REYNOLDS NUMBER APPROACHES I
*INFINITY FOR CONFIGURATION NUMBER',I2)
IF(II.EQ.2) WRITE(IH,17)CASYM1,F1,F12,CASYM3,F3,R34D12,FT
17 FORMAT(/,5X,'DH1 = ',F8.4,/,5X,'F1 = ',F8.4,/,5X,'F12 = ',F8.4,
*,5X,'DH3 = ',F8.4,/,5X,'F3 = ',F8.4,/,5X,
*,RE3/RE12 = ',F8.4,/,5X,'FT = ',F8.4)
IF(II.EQ.1) WRITE(IH,45)CASYM1,F1,F12
45 FORMAT(/,5X,'CH1 = ',F8.4,/,5X,'F1 = ',F8.4,/,5X,'F12 = ',F8.4)
IF(II.GT.2) WRITE(IH,26)CASYM1,F1,F12,CASYM3,F3,F34,R34D12,FT
26 FORMAT(/,5X,'CH1 = ',F8.4,/,5X,'F1 = ',F8.4,/,5X,'F12 = ',F8.4,
*,5X,'DH3 = ',F8.4,/,5X,'F3 = ',F8.4,/,5X,'F34 = ',F8.4,/,5X,
*,RE34/RE12 = ',F8.4,/,5X,'FT = ',F8.4)
C*****
C MAIN COMPUTATION
C
NN = 1
D12 = D12M
T1 = ((C1+C2)/C1)*D12
F1 = -C2/C1
D11 = T1
DINCR = DASYM1/ICJ.C
WRITE(6,18)
18 FORMAT(1H1)
WRITE(IH,77)II
77 FORMAT(/,10X,'VALUES FOR CONFIGURATION NUMBER ',II,/)
WRITE(IH,78)
78 FORMAT(1X,'REYNOLDS NUMBER(RET)',5X,'FRICTION FACTOR(FT)',/)
C

```



```

0109
0110
0111
0112
0113
0114
0115
0116
0117
0118
0119
0120
0121
0122
0123
0124
0125
0126
0127
0128
0129
0130
0131
0132
0133
0134
0135
0136
0137
0138
0139
0140
0141
0142
0143
0144

```

501 CONTINUE

C D1 = D11 - D1NCR
D11 = D1
D2 = (C1-T1)/F1

139 CONTINUE

C IF(D1.LE.0.0) GO TO 130
IF(D2.LE.C.C) GC TC 130
IF(D12.LE.0.0) GO TO 130

C RE2 GT 51,094

C RE12 = (D1**5.0)*D12/((S1**5.C)*(D2**6.0))
RE12 = RE12*(2.5*ALCG(D1/(2.*E)) + R)**10.C
RE12 = RE12/ACJLST**5
RE2 = (D2/D12)*RE12
IF(RE2.GT.51094.C) GO TO 135

C 1187.0 < RE2 < 51,094

C RE12 = (D1**4.0)*(D12)/((S**4.C)*(D2**5.0))
RE12 = RE12 * (2.5*ALCG(D1/(2.*E)) + R)**8.0
RE12 = RE12/ACJLST**4
RE2 = (D2/D12)*RE12
IF(RE2.GT.1187.C) GO TC 135

C RE2 LT 1187.0

C RE12 = 8.C*D1*D12/(ADJLST*D2*C2)
RE12 = RE12*(2.5*ALCG(D1/(2.*E)) + R)**2
RE2 = (D2/D12)*RE12

C 135 F12 = 2.*D12/D1
F12 = F12/(2.5*ALCG(D1/(2.*E)) + R)**2.
F12 = F12*ADJLST

```

C
C
C
C
RE1 = (D1/D12)*RE12
PR1 = 2.0*ADJUST/((2.5*ALCG(D1/(2.*E)) + R)**2)

RE2 = (D2/D12)*RE12
IF(RE12.LE.0.0) GC TO 130
IF(F12.LE.0.0) GC TO 130
ECN = SQRT(F12)*RE12/D12**1.5
RET = RE12
FT = F12
IF(II.NE.2) GC TO 28
PARM = D12*A3/D3
RF3 = ECN*D3**1.5/F3**0.5
V = (A12 + PARM*RE3/RE12)/AT
FT = F12*DHT/(C12*V*V)
RET = RE12*DHT*V/D12
28 CONTINUE
IF(II.NE.2) RE3 = 100.0
IF(II.EQ.1.OR.II.EC.2) WRITE(IM,23)RET,FT
23 FORMAT(6X,E11.4,T30,E11.4)
X12(1,NN) = ECN
X12(2,NN) = RE12
X12(3,NN) = F12
MAX12 = NN
NN = NN + 1
130 CONTINUE
IF(RE12.GT.50.0.AND.RE3.GT.50.0) GO TO 501
IF(II.LT.3) GC TO 105

SUB-AREA (3+4)
D34 = D34M
C
C
C
C
C

```

```

0131 T2 = ((C3+C4)/C3) * D34
0132 F2 = -C4/C3
0133 D33 = T2
0134 DINCR = CASYM3/100.C
0135 NN = 1
0136
0137
0138
0139
0140
0141
0142
0143
0144
0145
0146
0147
0148
0149
0150
0151
0152
0153
0154
0155
0156
0157
0158
0159
0160
0161
0162
0163
0164
0165
0166
0167
0168
0169
0170
0171
0172
0173
0174
0175
0176
0177
0178
0179
0180
0181
0182
0183
0184
0185
0186
0187
0188
0189
0190
0191
0192
0193
0194
0195
0196
0197
0198
0199
0200
0201
0202
0203
0204
0205
0206
0207
0208
0209
0210
0211
0212
0213
0214
0215
0216

```

C 502 CGTINUE
D3 = D33 - DINCR
D33 = D3
D4 = (D3-T2)/F2
D44 = D4
IF(D3.LE.0.0) GO TO 150
IF(D4.LE.0.0) GO TO 150
IF(D34.LE.0.0) GO TO 150
RE4 GT 51,C54
RE34 = (D3**5.0)*D34/((S1**5.0)*(D4**6.0))
RE34 = RE34*(2.5*ALCG(D3/(2.C*E)) + R)**10.0
RE34 = RE34/ACJUST**5
RE4 = (D4/D34)*RE34
IF(RE4.GT.51094.C) GO TO 155
1187.0 < RE4 < 51,C54
RE34 = (D3**4.0)*(D34)/((S**4.0)*(D4**5.0))
RE34 = RE34 * (2.5*ALCG(D3/(2.*E)) + R)**5.0
RE34 = RE34/ACJUST**4
RE4 = (D4/D34)*RE34
IF(RE4.GT.1187.0) GO TO 155
RE4 LT 1187.0
RE34 = 8.C*D3*C34/(ADJUST*C4*D4)
RE34 = RE34*(2.5*ALCG(D3/(2.*E)) + R)**2

```

0217
0218
0219
0220
0221
0222
0223
0224
0225
0226
0227
0228
0229
0230
0231
0232
0233
0234
0235
0236
0237
0238
0239
0240
J241
0242
0243
0244
0245
0246
0247
0248
0249
0250
0251
0252

```

RE4 = (C4/C34)*RE34
 155 F34 = 2.*C34/D3
 F34 = F34/(2.5*ALOG(D3/(2.*E)) + R)**2.
 F34 = F34 *ADJUST
 C
 RE3 = (D3/D34)*RE34
 FR3 = 2.0*ADJUST/((2.5*ALOG(D3/(2.*E)) + R)**2)
 C
 RE4 = (D4/D34)*RE34
 IF(RE34.LE.0.0) GO TO 150
 IF(F34.LE.C.C) GO TO 150
 EQN = SQRT(F34)*RE34/C34M**1.5
 X34(1,NN) = EQN
 X34(2,NN) = RE34
 X34(3,NN) = F34
 MAX34 = NN
 NN = NN + 1
 150 CONTINUE
 IF(RE34.GT.50.0) GO TO 502
 C
 C*****
 C
 CALC FT VS. RET FROM AREAS (1+2) & (3+4)
 C
 LOW12 = 2
 LOW34 = 2
 I = 2
 IF(X34(1,2).LT.X12(1,2)) GO TO 365
 360 I = I + 1
 IF(X12(1,2).LT.X34(1,1)) GO TO 360
 LOW34 = I
 GO TO 368
 365 I = I + 1
 IF(X34(1,2).LT.X12(1,1)) GO TO 365

```

C
LOW12 = I
368 CONTINUE
MAX12 = MAX12 - 1
MAX34 = MAX34 - 1
I = MAX12
369 IF (X34(1,MAX34).LT.X12(1,MAX12)) GO TO 374
370 I = I - 1
IF (X34(1,MAX34).GT.X12(1,I)) GO TO 37C
MAX12 = I
GO TO 376
374 I = MAX34
375 I = I - 1
IF (X12(1,MAX12).GT.X34(1,I)) GO TO 375
MAX34 = I
C
C
C
376 CONTINUE
MDIF12 = MAX12 - LOW12
MDIF34 = MAX34 - LOW34
IF (MDIF34.LT.MDIF12) GO TO 401
C
C
C
PARM2 = 2.*D12M*A34/C24M
IF (I1.EQ.4) PARM2 = PARM2/2.
DO 310 I = LOW12,MAX12
DIFF = 1C.E+6C
DO 300 J = LOW34,MAX34
DIFF1 = X12(1,I) - X24(1,J)
IF (ABS(DIFF1).LT.ARS(DIFF)) DIFF = DIFF1
IF (DIFF.EQ.(DIFF1) JSAVE = J
300 CCNTINUE
J = JSAVE
JV = J - 1
IF (DIFF.LT.0.0) JV = J + 1
XC = X34(1,JV) - X34(1,J)
0253
0254
0255
0256
0257
0258
0259
0260
0261
0262
0263
0264
0265
0266
0267
0268
0269
0270
0271
0272
0273
0274
0275
0276
0277
0278
0279
0280
0281
0282
0283
0284
0285
0286
0287
0288

```

```

0289 FRACT = DIFF/XC
0290 DE = (X34(1,JV) - X34(1,J))*FRACT
0291 EQN = X34(1,J) + CE
0292 DR = (X34(2,JV) - X34(2,J))*FRACT
0293 RE34 = X34(2,J) + DR
0294 DF = (X34(3,JV) - X34(3,J))*FRACT
0295 F34 = X34(3,J) + DF
C
0296 V = (A12 + PARM2*RE34/X12(2,I))/AT
0297 FT = X12(3,I)*CHT/(D12M*V*V)
0298 RET = X12(2,I)*CHT*V/D12M
C
0300 WRITE(IH,23)RET,FT
C 310 CONTINUE
C GO TO 411
C
C
C 401 CONTINUE
PARM2 = C34M*A12/D12M
PARM3 = 2.
IF(II.EQ.4) PARM3 = PARM3/2.
DO 410 I = LOW34,MAX34
DIFF = 10.E+60
DO 40C J = LOW12,MAX12
DIFF1 = X34(1,I) - X12(1,J)
IF(ABS(DIFF1).LT.ABS(DIFF)) DIFF = DIFF1
IF(DIFF.EQ.DIFF1) JSAVE = J
400 CONTINUE
J = JSAVE
JV = J - 1
IF(DIFF.LT.0.0) JV = J + 1
XC = X12(1,JV) - X12(1,J)
FRACT = DIFF/XC
DE = (X12(1,JV) - X12(1,J))*FRACT
EQN = X12(1,J) + DE

```

0289
0290
0291
0292
0293
0294
0295
0296
0297
0298
0299
0300
0301
0302
0303
0304
0305
0306
0307
0308
0309
0310
0311
0312
0313
0314
0315
0316
0317
0318
0319
0320
0321
0322
0323
0324

```

0325 DR = (X12(2,JV) - X12(2,J))*FRACT
0326 RE12 = X12(2,J) + CR
0327 DF = (X12(3,JV) - X12(3,J))*FRACT
0328 F12 = X12(3,J) + DF
0329
0330 V = (PARM3*A34 + PARM2*RE12/X34(2,I))/AT
0331 FT = X34(3,I)*CH1/(D34M*V*V)
0332 RET = X34(2,I)*DHT*V/D34M
0333
0334 WRITE(IW,23) RET,FT
0335
0336
0337
0338
0339
0340
0341
0342
0343
0344
0345
0346 SUBROUTINE AREAL(IW,II,RC,RP,A12,A3,AT,C1,C2,C3,D12,D3,DHT)
0347 WRITE(IW,70)II
0348 TO FORMAT(IH1,IOX,'VALUES FROM SUBROUTINE AREAL FOR CONFIGURATION NUM
0349 *BER',I2)
0350
0351 PI = 3.1415927
0352 DP = 2.*RP
0353 DC = 2.*RC
0354 C1 = 5.*PI*RC
0355 C2 = PI*DP
0356 C3 = PI*RC
0357 A3 = (SQRT(3.))-0.5*PI)*RC*RC
0358 IF(II.EQ.2) A3 = 3.*1.5*RP*RP/16. - PI*RC*RC/2.
0359 AT = PI*(RP*RP - 3.*RC*RC)
0360 A12 = AT - A3

```

```

0361 D12 = 4.*A12/(C1 + C2)
0362 D3 = 4.*A3/C3
0363 DHT = 4.*AT/(C1 + C2 + C3)
0364 WRITE(IW,20)RC,RP,A12,C1,C2,D12,DHT,AT
0365 FORMAT(5X,'RC = ',F8.4,/,5X,'RP = ',F8.4,/,5X,
0366 '*A12 = ',F8.4,/,5X,'C1 = ',F8.4,/,5X,'C2 = ',F8.4,/,5X,
0367 '*D12 = ',F8.4,/,5X,'DHT = ',F8.4,/,5X,'AT = ',F8.4)
0368 IF(II.EQ.1) GO TO 40
0369 WRITE(IW,30)A3,C3,C3
0370 FORMAT(5X,'A3 = ',F8.4,/,5X,'C3 = ',F8.4,/,5X,'D3 = ',F8.4)
0371 40 CONTINUE
0372 RETURN
0373 END
0374 SUBROUTINE AREA2(IW,II,RC,RP,A12,A34,AT,C1,C2,C3,C4,D12,C34,DHT)
0375 WRITE(IW,70)II
0376 FORMAT(IH1,1CX,'VALLES FROM SUBROUTINE AREA2 FOR CONFIGURATION NUM
0377 *BER',I2)
0378 DC = 2.0*RC
0379 DP = 2.0*RP
0380 PI=3.141593
0381 RADDEG = 180.0/PI
0382 DETERMINE AREAS A12 & A34
0383 Y = RP - RC
0384 H = (Y*Y - RC*RC)**0.5
0385 THETA = ATAN(H/RC)
0386 DTHETA = THETA*RADDEG
0387 AC = PI * RC**2.
0388 AA = ((PI - THETA)/PI)*AC
0389 ATR = H*RC
0390 AN = ATR + AA
0391 ALPHA = PI - 2.*THETA
0392 DALPHA = ALPHA*RADDEG
0393 AP = PI * RP * RP
0394 ASL = (ALPHA*AP)/(2.*PI)
0395 A34 = ASL - AN
0396 AT = (PI/4.0)*(DP*DP-3.0*CC*CC)

```

C


```

0397 A12 = AT - 2.*A34
0398 DETERMINE CIRCUMFERENCES C1, C2, C3, C4
0399 CP = 2.*PI*RP
0400 C4 = ALPHA * FP
0401 C2 = CP - 2.*C4
0402 CC = 2. * PI * RC
0403 C3 = ((PI-THETA)/PI) * CC
0404 C1 = 3.*CC - 2.*C3
0405 IF(II.EQ.3) GO TO 10
0406 AT = AT - (SQRT(3.)-C.5*PI)*RC*RC
0407 A12 = AT - A34
0408 C1 = 11.*PI*RC/3.
0409 C2 = CP - C4
0410
10 CONTINUE
C CALCULATE HYDRAULIC DIAMETERS D12 & D34
D12 = (4.*A12)/(C1+C2)
D34 = (4.*A34)/(C3+C4)
DHT = (DP*DP-3.0*CC*DC)/(CP+3.0*DC)
WRITE(IW,520)A12,A34
WRITE(IW,521)C1,C2,C3,C4,CP,CC,D12,D34
520 FORMAT(/,5X,'A12 = ',F11.5/,5X,'A34 = ',F11.5)
521 FORMAT(/,5X,'C1 = ',F11.5/,5X,'C2 = ',F11.5/,5X,'C3 = ',F11.5,
*/,5X,'C4 = ',F11.5/,5X,'CP = ',F11.5/,5X,'CC = ',F11.5/,5X,
*,'D12 = ',F11.5/,5X,'D34 = ',F11.5)
WRITE(IW,500)AT,CT
500 FURMAT(5X,'AT = ',F11.5/,5X,'DHT = ',F11.5)
RETURN
END
02 10.25 4.135 1.5 .1
1111 .89
1 10.25 3.955 1.5 .1
.89

```